Quantifying the Effects of Water Management Decisions on Streambank Stability

by

Quan Wei

A thesis

presented to the University of Waterloo

in fulfillment of the

thesis requirement for the degree of

Master of Science

in

Earth Science (Water)

Waterloo, Ontario, Canada, 2022

Author's Declaration

I hereby declare that I am the sole author of this thesis. This is a true copy of the thesis, including any required final revisions, as accepted by my examiners. I understand that my thesis may be made electronically available to the public.

Abstract

Streams continuously change due to natural processes and human activities, significantly affecting streambank erosion and stability. These changes cause severe environmental issues, including sedimentation of reservoirs, contamination of streams, loss of productive land, and damage to infrastructure. Many factors affect streambank erosion and stability, including hydrological conditions of the stream and streambank environment, which are often controlled by environmental structures and water management decisions. Much is known about hydrology and water management, as well as hydrology and streambank stability. However, there is still little research that considers the connection between water management and streambank stability. The objective of this work is to quantify how water management decisions, particularly reservoir operations, affect streambank stability.

A module was developed to estimate streambank stability using a factor of safety approach and uses results from an established integrated hydrologic model to characterize hydrologic conditions. This module is validated and then demonstrated using model results from the Lower Republican River Basin in Kansas, USA. Results applied at the LRRB indicated that several water management decisions may negatively affect streambank stability by changing pore water pressure, the weight of the streambank soil, and the status of erosion.

Acknowledgments

Firstly, I would like to thank my supervisor, Dr. Andrea Brookfield, for giving me the chance to work with her and for her kindness. I appreciate her guidance and help so I can successfully complete my project and thesis.

Appreciate the support and assistance by Hydrogeosphere distributed by Aquanty Inc.

I am thankful for the suggestions and support of my committee members, Dr. David Rudolph and Dr. Andre Unger.

Also, I am grateful to Dr. Tony Layzell for providing the field data and assisting me in completing my thesis project.

Finally, I will thank my friends and my family for their help, support, and encouragement during my graduate studies, especially during the pandemic of COVID-19.

Table of Contents

List of Figures

List of Tables

Chapter 1.0: Introduction

Continued urbanization, including the construction of large-scale water conservancy projects and changing hydrologic conditions due to climate change, have caused the sedimentary environment of rivers to undergo tremendous change. This includes changes to the timing and volume of sediment loads, which are the eroded solid matter transported through rivers, and are an essential part of fluvial systems (Zhang, 2008). In addition, human activities, such as land use changes and reservoir construction, can significantly affect a river's sediment loads. For example, the construction of dams will significantly decrease the sediment loads downstream as the water slows down and loses energy in the reservoir, causing deposition (Yang, 2007). Likewise, groundwater pumping and the subsequent decline in groundwater levels can significantly affect streambank stability through changes in pore pressure which can stabilize or destabilize streambank materials (Casagli, 1999). Large volumes of water and faster water flow due to heavy precipitation or reservoir releases can also affect pore water pressure resulting in changes in streambank stability. For example, groundwater tables will increase during high stream flow events, causing changes to the lateral seepage and capillary forces and affecting the matric suction along the bank. The changes in matric suction in response to a flow event will vary depending on different bank conditions, such as soil type, groundwater level, topography, and hydraulic properties (Casagli, 1999).

Streambank instability can be the source of many serious environmental problems. The soil from the failed streambanks may contain bacteria and contaminants that can cause economic and health issues when transported downstream. For example, nutrient-rich bank soil and sediment loads transported to reservoirs and streams may support algal bloom growth, which can be harmful to ecologic and human health, and sedimentation of reservoirs decreases their ability to mitigate floods or store water for downstream use (Preece et al., 2021, Fatiha, 2020). Therefore, understanding and quantifying sediment loads and streambank stability, including their relation to hydrologic conditions and water resource management decisions, is necessary for maintaining the human, ecologic, and economic health of river systems and their local environments.

Hydrologic models are one of the most common methods to support water management decisions (Midgley, 2012). Several models are available for simulating reservoir management strategies (e.g., Asselt et al., 2001; Green, 1976); however, a model that can consider water management and streambank stability is lacking. Although many researchers study stream erosion and streambank stability (e.g., Midgley, 2012; Chu-Agor et al., 2008), models and research about the relationship between streambank stability and water management decisions are limited. Recently, Brookfield and Layzell (2019) built an integrated hydrological model to simulate and predict both natural and engineering hydrologic conditions and fluvial erosion and applied it to the Lower Republican River Basin (LRRB), United States. Fluvial erosion was simulated using the

excess shear stress approach based on the results of an existing hydrologic framework which coupled a physically based integrated hydrologic model, HydroGeoSphere (HGS; Therrien et al., 2007), with a surface water operations model, Operational Analysis and Simulation of Integrated Systems (OASIS; Hydrologic, 2009). This model was used to assess water management strategies for their ability to reduce both water shortages and fluvial erosion in the LRRB. The current research builds upon the work by Brookfield and Layzell (2019) to include an estimate of streambank stability.

1.1 Objective

As previously indicated, groundwater, surface water, and their combined effects can cause streambank instability. Some models, such as MODFLOW (Langevin et al., 2017), only simulate hydrologic conditions of the subsurface, while models such as RiverWare (Valerio et al., 2010.; Qiu et al., 2019) only simulate hydrologic conditions on the surface. A comprehensive hydrological model that considers groundwater and surface water is essential to studying streambank stability. While many studies have investigated water management and streambank stability independently (e.g., Asselt et al., 2001; Green, 1976; Midgley, 2012; Chu-Agor et al., 2008), very few have considered them together. Thus, the objective of this research is to investigate how streambank stability may change due to water management decisions, creating a framework to help support decisions that would reduce both water shortages and erosion. This objective is met through the development of a streambank stability model that uses the results of the

hydrologic model, Hydrogeosphere, to estimate streambank stability. Using this model, the effects of different hydrologic conditions resulting from different hydrologic and climate conditions on both water availability and streambank stability are studied.

Chapter 2.0: Previous Research

Significant research has studied components of the flow and transport of water and sediment through the surface and subsurface hydrologic systems, including integrated hydrologic models, surface water operation models, streambank stability and sediment transport models, and models that estimate streambank factors of safety (Langevin et al., 2017; Fredlund et al., 2018; Diersch., 2014; Hydrologic, 2009; Valerio et al., 2010.; Qiu et al., 2019; Midgley, 2012; Chu-Agor et al., 2008). These models study components of the flow and sediment transport system but do not integrate across the entire terrestrial water cycle. Coupling these models is the foundation of this work, and a review of some of these models is provided below.

2.1 Integrated Hydrologic Models

Surface water and groundwater are constantly interacting, and shallow groundwater and deep groundwater are continually being exchanged. Due to the complexity of the relationship between surface water and groundwater, many early models and studies treated the flow and transport processes of surface water and groundwater independently. Models that simulate groundwater flow and transport include MODFLOW, FEHIM, and FEFLOW (Langevin et al., 2017; Fredlund et al., 2018; Diersch., 2014). Models that simulate surface water flow and transport include OASIS (Hydrologic, 2009), RiverWare (Valerio et al., 2010.; Qiu et al., 2019), and SWAT (Kim et al., 2008). More recently,

integrated hydrologic models have been developed to represent flow through the entire terrestrial water system, including surface water and groundwater, as needed for this work, such as HydroGeoSphere, ParFlow, and GSFLOW (e.g., Brunner, 2012; Maxwell et al., 2015; Taie Semiromi et al., 2019). These models are discussed in more detail below.

2.1.1 HydroGeoSphere

Hydrogeosphere (HGS) is a commonly used integrated hydrologic model developed at the University of Waterloo and distributed by Aquanty Inc. (Therrien et al., 2010). HGS integrates surface water and groundwater, and it can be used to solve a range of fundamental hydrological problems from simple to complex systems. The primary governing equations used in HGS are the 3D formulation of Richards' equation and the 2D diffusive-wave Saint Venant equation for groundwater and surface water, respectively (An & Yan, 2018). In addition, HGS can simulate variable-density flow and transport, first-order decay reactions, reactive chemical species transport, heat transport, and flow through fractures, among other processes (Brunner & Simmons, 2012). HGS has been used for water management in several studies, including Brookfield and Layzell (2019) and Li et al. (2008). Li et al. (2008) used HGS to assess the possible impacts and benefits of various water management scenarios on surface water and groundwater at Duffins Creek, Ontario, Canada.

2.1.2 ParFlow

ParFlow is another integrated hydrologic model that simulates the integrated surface and subsurface hydrologic system (Kollet & Maxwell, 2006). ParFlow can capture different soil characteristics, topography, and aquifer characteristics under complex surface and subsurface circumstances. Similar to HGS, ParFlow uses Richards' equation to simulate the groundwater flow, although ParFlow uses the kinematic-wave version of the Saint Venant equation to calculate surface water flows and transport (Benjamin et al., 2020) and has been used to support water management decisions. For example, Shadi et al. (2018) developed a ParFlow model to simulate groundwater flow and contaminant transport in a basin in Jordan undergoing severe groundwater depletion to support water management decisions.

2.1.3 GSFLOW

GSFLOW is an integrated hydrologic model developed by the United States Geological Survey (USGS) based on the commonly used groundwater flow model, MODFLOW, and USGS Precipitation-Runoff Modeling System (PRMS-V; Harbaugh, 2005). GSFLOW is a coupled model that can be used to simulate saturated and unsaturated flows; subsurface flows in different materials, and transportation in rivers and lakes by solving the Saint-Venant kinematic-wave equation and 3D Richards' equation in an iteration loop

(Markstrom et al., 2016; Steven et al., 2005). Related to water management, Surfleet & Tullos (2015) used GSFLOW to simulate different hydrological conditions at the Santiam River basin in Oregon, USA, and used the results to predict and study the uncertainty caused by climate change in 2013.

2.2 Surface Water Operation Models

Surface water operation models simulate management infrastructures, such as reservoir management and water distribution systems. As opposed to the hydrologic models governed by physics, the surface water operations models are often governed by a combination of physical constraints and the rules and regulations governing the management systems' operation (Valerio et al., 2010). They can be a sufficient basis for water resources management decisions where these structures regulate water distribution. They are often linked to a surface water routing package to account for water transport between surface water bodies and other points of interest. Examples of these models include OASIS (Hydrologic, 2009) and RiverWare (Valerio et al., 2010; Qiu et al., 2019).

2.2.1 OASIS

OASIS is a linear optimization model that can simulate rules and guidelines used to operate reservoirs and other water management structures (McKinney, 2004). It uses a linear optimization solution method and simulates stream flow using water routing techniques. OASIS has been coupled with many other models, including HGS, to create

an integrated model to solve various problems, including links to groundwater quantity and water quality (Brookfield et al., 2017; Brookfield & Layzell, 2019). OASIS is widely used for water management across North America, including the South Florida Water Management District, the Delaware River, the Roanoke River, the Kansas River, the Rio Grande, and the South Fork of the American River (McKinney, 2004).

2.2.2 RiverWare

RiverWare is an integrated river system model similar to OASIS that combines physical processes, manual operations, and strategic logic. In RiverWare, many manmade and natural water bodies can be simulated, such as reservoirs, natural river sections, manmade canals, and aquifers. Additionally, RiverWare can simulate integrated rule-based operations based on the rights and laws of the study area (Valerio et al., 2010). RiverWare uses different methods for each object; for example, for modeling reservoirs, RiverWare uses the mass balance approach and other different rule-based simulation approaches to create a framework for users to simulate complex objects in streams and water cycles (Center for Advanced Decision Support for Water and Environmental Systems, 2019; Basheer & Elagib, 2018). Qiu et al. (2019) applied RiverWare to the Yakima River basin in Washington, USA, to study the effects of water management strategies, reservoir operation decisions, and irrigation activities on the water cycle. They compared several modeling methods and found that coupling RiverWare and SWAT was

the optimal approach for simulating water management scenarios and demonstrated the importance of integrating irrigation strategies into hydrological models.

2.3 Streambank Erosion and Stability Models and Methods

Streambank erosion and stability models focus on the physical processes within and along the streambeds. These models consider the effects of water levels, streambank properties, and pore pressures, amongst other parameters and processes, on the stability of streambanks. Examples of streambank erosion models include BSTEM (Midgley, 2012) and SLOPE/W (Chu-Agor et al., 2008), and several Factor of Safety methods (Simon et al., 2000; Langendoen et al., 2000; Osman and Thorne, 1998).

2.3.1 BSTEM

One of the most common erosion models is the Bank Stability and Toe Erosion Model (BSTEM), developed at the U.S. National Sedimentation Laboratory (Midgley, 2012; Duan et al., 2018; Okeke et al., 2019; Fox et al., 2011). BSTEM not only considers both streambank stability and streambank toe erosion but also studies the relationships between them based on the excess shear stress equation and a non-linear mechanistic model (Klavon et al., 2017). BSTEM uses limit equilibrium methods and considers horizontal and vertical layers to simulate streambank stability and toe erosion (Midgley, 2012). Mohammed-Ali et al. (2019) used BSTEM to simulate the streambank instabilities caused by long-term fluctuations of water releases along 130 km of the streambanks near

Bagnell Dam, Missouri, USA. Langendoen et al. (2014) studied the Debre-Mewi watershed, Ethiopia, focusing on expanding that valley and keeping banks stable and safe.

2.3.2 SLOPE/W

SLOPE/W is also widely used for simulating streambank stability and is based on limit equilibrium theory (Chu-Agor et al., 2008). It simulates the stability of different slip surfaces, with varying characteristics of soil, and pore pressures, amongst other factors. SLOPE/W can simultaneously simulate thousands of slip surfaces and approximates the possibility of displacement of the slip surface (Chu-Agor et al., 2008). Borg (2014) used this model to simulate the streambank stability of the Winooski River, Vermont, the USA, using effective strength in soils below the groundwater level and parameters of increased unit weight and effective strength in the soil above the groundwater level. This research concluded that rapid drawdown events could cause streambank instabilities.

2.3.3 Factor of Safety Methods

In addition to streambank erosion and stability models, models that estimate factors of safety (F_S) for streambank stability are widely used. The factor of safety can indicate streambank stability by calculating the balance between driving forces and resisting forces for a streambank reach (Bankhead et al., 2013). If F_S is less than 1, the driving

force is larger than the resisting force so that streambank instability may occur; however, if F_S is larger than 1, the streambank is stable. When F_S is equal to 1, it is generally considered an unstable streambank that will fail soon without intervention (Simon et al., 2000). F_S methods include Horizontal Layer Method (Simon et al., 2000), Vertical Slides Method (Langendoen et al., 2000), and Osman and Thorne's (1998) Approach.

2.3.3.1 Horizontal Layer Method (Simon et al., 2000)

According to Simon et al. (2000), the factor of safety (F_S) can be calculated for horizontal layers using the following equation:

$$Fs = \frac{\sum c_i' L_i + (S_i \tan \varphi_i^b) + [W_i \cos \beta - U_i + P_i \cos(\alpha - \beta)] \tan \varphi_i'}{\sum W_i \sin \beta - P_i \sin(\alpha - \beta)} \qquad (1)$$

Where c' is the effective cohesion, L_i is the length of the failure plane incorporated within the i^{th} layer; S is the force produced by matric suction on the unsaturated part of the failure surface, φ' is the effective friction angle, φ^b is an angle indicating the increase in shear strength for an increase in matric suction, W is the weight of the failure block, α *and* β are the angles of the failure plane, U is the hydrostatic-uplift force on the saturated portion of the failure surface, P is the hydrostatic-confining force due to external water level (Simon et al. 2000).

2.3.3.2 Vertical Slices Method (Langendoen et al., 2000)

Similarly, Langendoen (2000) provided another equation to calculate F_S based on vertical slices:

$$F_s = \frac{\cos\beta \sum_{i=1}^{N} (L_i c'_i + N_i \tan \phi'_i - U_i \tan \phi_i^b)}{\sin\beta \sum_{i=1}^{N} N_i - F_w} \quad (2)$$

Where β is the angle of the failure plane, L_i is the length of the slice base, c' is the effective cohesion, N_i is the normal force on the base of the slice, U_i is the porewater force on the base of the slice, ϕ'_i is the effective angle of internal friction, ϕ^b_i is an angle indicating the increase in shear strength for an increase in matric suction, F_w is hydrostatic force per unit channel length exerted by surface water on the vertical section of the slip surface (Langendoen, 2000).

2.3.3.3 Osman and Thorne (1998) Approach

Osman and Thorne (1998) also provide an estimate of streambank stability using a factor of safety that is different from the vertical slides and horizontal layer methods. In their equations, F_S is equal to the ratio of resisting force (F_R) and driving force (F_D), and the complete equation for calculating the factor of safety is given by:

$$F_S = \frac{\frac{(H-y)c'}{\tan\beta} + \frac{\gamma}{2}\left(\frac{H^2 - y^2}{\tan\beta} - \frac{H'^2}{\tan i}\right)\cos\beta \tan\phi'}{\frac{\gamma}{2}\left(\frac{H^2 - y^2}{\tan\beta} - \frac{H'^2}{\tan i}\right)\sin\beta} \quad (3)$$

where H is the bank height above the streambed, y is the depth of tension cracking, c' is the effective cohesion, γ is the specific weight, i is the initial bank angle, β is the angle the failure plane makes with the horizontal, ϕ' is the effective friction angle, and H' is the bank height above the failure point (Osman & Thorne, 1998; Admiraal, 2007).

All of these methods have been extensively used and verified to provide accurate estimates of streambank stability, and a primary consideration in method selection is the required data and measurements, in addition to the computational complexity of the coupled model. As the purpose of this research is to develop a modeling framework that provides an initial estimate of streambank stability given hydrologic conditions driven by water management decisions, it was concluded that a factor of safety approach was the most appropriate.

2.3.4 Method Selection

There are two main types of streambank instabilities or failure: 1) For streambank angles of less than 60 degrees, the failure surface is curved, and these streambanks fail due to rotational slip (Langendoen, 2000; Figure 1a); 2) For steep banks with angles greater than 60 degrees, the failure surfaces will occur along planar surfaces causing planar failures (Figure 1b). As planar failure is one of the most common types of streambank failure (Langendoen, 2000), it will be the focus of this research.

Three factors of safety approaches were described in the previous section. Simon et al. (2000) and Osman and Thorne (1998) use similar methodologies; however, the Osman and Thorne (1998) approach does not consider hydrological characteristics, including pore water pressure, which makes it unsuitable for this work. While the Horizontal Layer Method (Simon et al., 2000) does incorporate hydrologic conditions, the data

requirements are more difficult to collect in the field, particularly at the site we will use for demonstration. The Langendoen et al. (2000) approach includes pore water pressure, simulates planar failures, and uses data that is more readily available, particularly at our demonstration site. Both the Langendoen (2000) and Simon et al. (2000) methods are simplified for hydrostatic conditions; therefore, they both have errors and uncertainty associated with this assumption. Given that the goal of the model framework is to provide a preliminary estimate of streambank stability given hydrologic conditions, this, in addition to other uncertainties associated with the parameterization and model development, is considered acceptable for this work. Based on all these considerations, the Langendoen et al. (2000) approach (equation 2) was selected for this research.

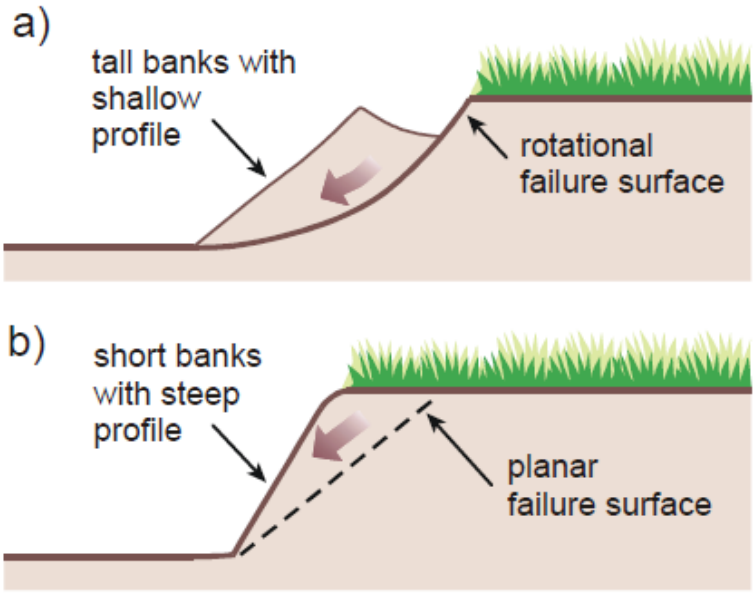

Figure 1 Failure Types (Langendoen et al., 2000)

Chapter 3.0: Model development and Validation

To fully consider the impacts of hydrological behavior and water management decisions on the stability of streambanks, a streambank stability module was developed that can use the output from an HGS simulation to represent integrated hydrologic conditions such as pore water pressure and surface water levels.

3.1 Model Development

Streambank stability is estimated using the Vertical Slides Method (Langendoen et al., 2000). In this approach, streambanks are separated into several vertical layers, with some layers partly or completely below the water table (Figure 2). Figures 3 and 4 show the relationships between the forces acting on a streambank, with normal forces, shear forces, and gravity acting in the vertical direction, and hydrostatic forces with components perpendicular to gravity. The weight and corresponding vertical gravitational force is the

main driving force in a failure, and the normal force, shear stress, and hydrostatic forces are the forces that will resist the failure.

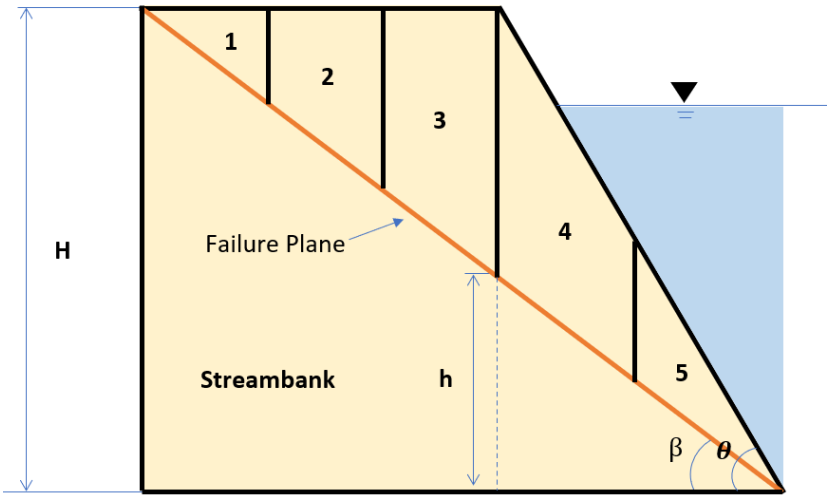

Figure 2: Simplified streambank cross-section split into 5 slices, where H is the height of the streambank, β is the angle of the failure plane, and θ is the angle of the streambank.

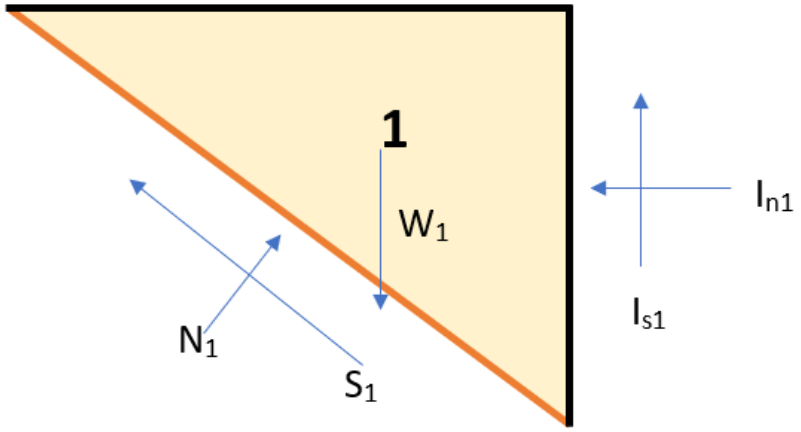

Figure 3: Force on streambank cross section (Slice 1), where Ni is the normal force, S is the shear force on the slide's base, W is the weight, Is is the vertical interslice shear force, and In is the horizontal interslice shear force.

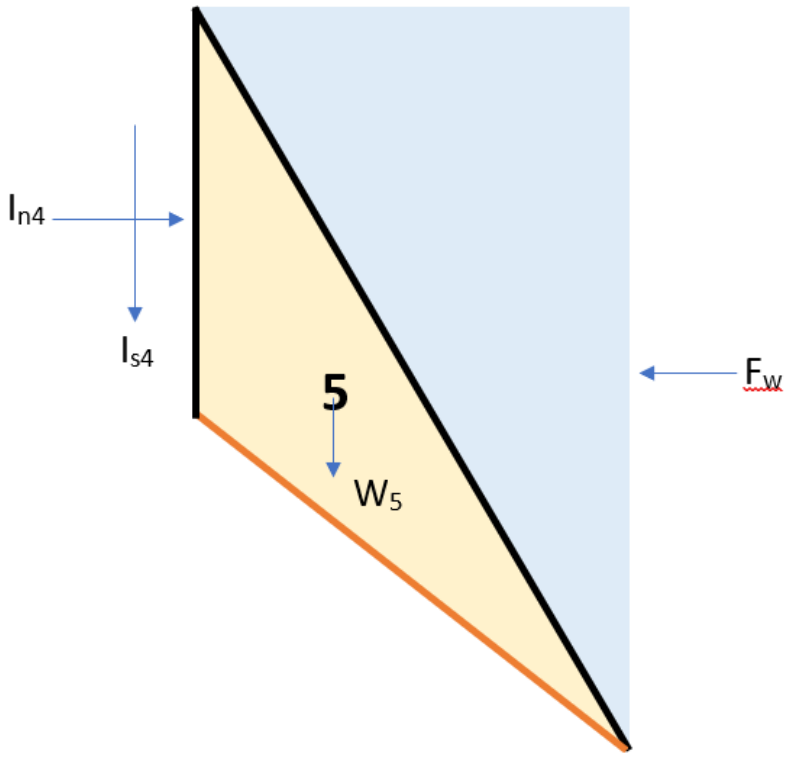

Figure 4: Force on streambank cross section (Slice 5), where Fw is the hydrostatic force.

To simplify the streambank, it was divided into five vertical layers, with each layer having a default width of 1 m. In Langendoen et al. (2000), three layers were used, but we have expanded to five layers for increased accuracy; however, more layers also increase the computational demand of the model. Future research will consider the trade-offs between increased accuracy and computational demand because of increased layers. According to the reasons indicated above, the layers here are simplified as homogeneous also to reduce computational demand, but future work will assess the benefits of heterogeneous layers. These homogeneous layers will further increase the error and uncertainty of model results, which will also be assessed in future work.

Each layer is calculated separately in the model using equations 4 to 11 (described in more detail below), and then the results are combined using equation 12. Following previous research, the calculation of F_S using the Vertical Slides Method is a 4-step iterative process, as outlined below:

Step 1: Calculate the normal force (N_j) acting at the base of a slice using vertical forces:

$$N_j = \frac{W_j}{\cos \beta} \tag{4}$$

Where β is the failure-plane angle (degree), and W_j is the weight of the slice (N).

The weight of a slide can be calculated by:

$$W_j = \gamma * V_j \tag{5}$$

Where γ is the bulk density of streambank soil (kg/m^3), and V_j is the volume of each layer (m^3). Bulk density can be determined using:

$$\gamma = \gamma_w \frac{G + e \times S}{1 + e} \tag{6}$$

Where γ_w is the density of water (kg/m^3), G is the specific weight of soil (unitless), e is the void ratio (unitless), and S is the saturation of that soil (unitless).

Following Figure 2, the streambank was simplified and separated into five vertical layers, with each layer having different volumes with a unit width (W_a (m); Table 1). Appendix A has the derivation for each vertical layer's volume.

Table 1: Volumes for each vertical layer

Number of Layers	Volumes (m^3)
1	$(H-h)^2/(18*\tan(\beta))*W_a$
2	$(H-h)^2/(6*\tan(\beta))* W_a$
3	$5*(H-h)^2/(18*\tan(\beta))* W_a$
4	$3*(H-h)*(H)/(\tan(\theta)*8)* W_a$
5	$(H-h)*(H)/(\tan(\theta)*8)* W_a$

The normal force calculated using equation 4 is for the first iteration, and the initial value of F_S is given as 1.

Step 2: Calculate the horizontal interslice normal force I_{nj}:

$$I_{nj} = I_{nj-1} - \left(c_j' L_j + S_j \tan \emptyset_j^b - U_j tan\emptyset_j'\right)\frac{cos\beta}{F_s} + N_j\left(sin\beta - \frac{cos\beta tan\emptyset_j'}{F_s}\right) \quad (7)$$

Where c_j' is the effective cohesion (Pa), L_j is the length of the slice base (m), S_j is the shear force mobilized at the base of the slice (N), ϕ^b_j is an angle indicating the increase in shear strength for an increase in matric suction (degree), U_j is the porewater force on the base of the slice (N), ϕ'_j is the effective angle of internal friction (degree), β is the angle of the failure plane (degree), F_S is the initial value of the factor of safety (unitless), and N_j is the normal force (N).

In equation 7, the shear force (S_j) and porewater force (U_j) can be calculated using equations 8 and 9:

$$U_j = \gamma_w\left(z_j - z_g\right)L_j \times W_a \quad (8)$$

$$S_j = \frac{1}{F_s}\left(L_j c'_j + N_j tan\emptyset'_j - U_j tan\emptyset^b_j\right) \quad (9)$$

Where γ_w is the unit weight of water (kg/m^3), z_j is the elevation at the center of the base (m), z_g is the groundwater level (m) (Langendoen, 2000), W_a is the width of the streambank (m) and was set to 1 m in this research, so L_j x W_a in this equation will be an area with a unit width.

Step 3: Use the horizontal interslice normal force to calculate the interslice shear forces (I_{sj}):

$$I_{sj} = 0.4\, I_{nj} \sin\left(\frac{\pi L_j}{\sum L_j}\right) \quad (10)$$

Step 4: Calculate the new normal force (N_j) using equation 11:

$$N_j = \frac{W_j + I_{sj-1} - I_{sj} - sin\beta\left(\frac{c'_j L_j + S_j tan\emptyset^b_j - U_j tan\emptyset'_j}{F_s}\right)}{cos\beta + \frac{tan\emptyset'_j sin\beta}{F_s}} \quad (11)$$

The steps described above are for the first iteration, and then we will use the new normal force to calculate the factor of safety using the equilibrium method as defined by Simon et al. (2006):

$$F_s = \frac{\cos\beta \sum_{j=1}^{N}(L_j c'_j + S_j tan\emptyset^b_j + (N_j - U_j)\tan\phi'_j)}{\sin\beta \sum_{j=1}^{N} N_j - F_w} \quad (12)$$

Where F_w is the hydrostatic force on the vertical surface (N) since we assume the groundwater level will not be higher than the ground surface (not flooding conditions), the pore water pressure at the top of the streambank can be assumed as 0, and pore water pressure (P_{wb}) at the bottom can be determined by the groundwater level (Pa):

$$P_{wb} = WL \times \rho \times g \quad (13)$$

Where WL is the groundwater level (m), the porewater force of the whole streambank (N) can be determined as:

$$F_w = (P_{wb}) \times \frac{WL}{2} \quad (14)$$

As previously indicated, this reflects hydrostatic conditions, likely not representative of real-world conditions. However, as discussed in Section 2.3.4, we feel that the results of this model would still provide an informative preliminary assessment of streambank stability.

For the next step, three different β values were tested to determine the lowest F_S value in one simulation following the method used in HEC-RAS (US Army Corps of Engineers, 2015). This method was replicated in the model developed as part of this work. First, three angles are selected: the minimum bracket angle (ϕ/2), which is the green point in Figure 5; the maximum bracket angle (average angle of streambanks), which is the purple point; and the first guess angle (45+ ϕ/2), which is the blue point. These angles are referred to as x_1, x_2, and x_3, respectively. If the average angle of streambanks is smaller than 45, the model will keep the same minimum bracket angle (x_1) and the maximum bracket angle (average streambank angles); but the first guess angle will be the average of minimum and maximum bracket angles. As shown in Figure 5, the red point is the factor of safety calculated by the model using the lowest failure angle determined by the best-fitted parabola, where the goal is to locate the lowest factor of safety as indicated by the

orange circle in Figure 5a. If the difference between the red point (model results) and the orange circle (determined by the best-fitted parabola) is less than 5%, then it is assumed that the red point is representative of the lowest factor of safety; however, if the difference is larger than 5%, the new factor of safety results (red point) replaces either the maximum angles or minimum angles in the model (Figure 5b; depending on if it is higher or lower than the first guess angle), and the previous steps are repeated until the lowest factor of safety is identified.

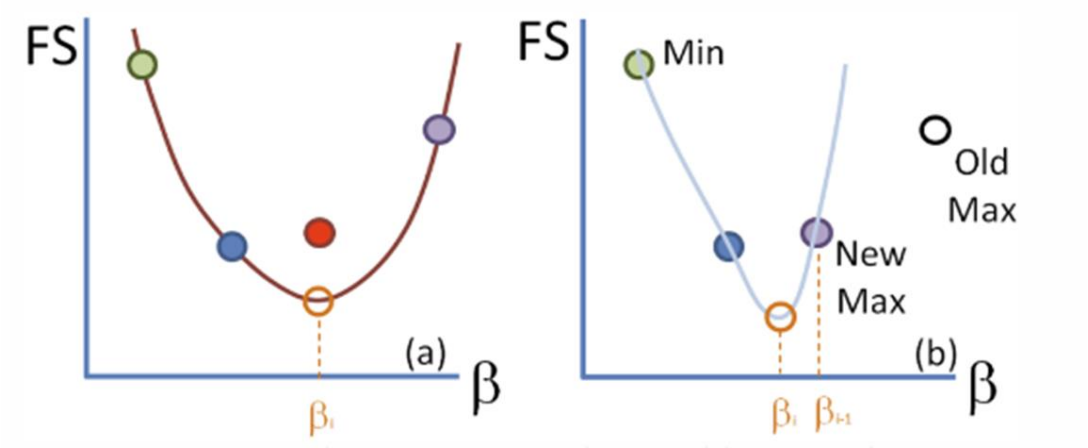

Figure 5: HEC-RAS Method (US Army Corps of Engineers, 2015)

Using the method described above, F_S is calculated at the minimum, maximum, and current estimated lowest angle, given by y_1,y_2, and y_3, respectively. Coupled x and y values are then inserted into a coordinate system, assuming a function of the best-fitted parabola:

$$Y = aX^2 + bX + c \tag{15}$$

Where the value of a, b and c can be determined as:

$$a = \frac{(y_2 - y_1)(x_3 - x_2) - (y_3 - y_2)(x_2 - x_1)}{(x_2^2 - x_1^2)(x_3 - x_2) - (x_3^2 - x_2^2)(x_2 - x_1)} \quad (16)$$

$$b = \frac{y_2 - y_1 - a(x_2^2 - x_1^2)}{x_2 - x_1} \quad (17)$$

$$c = y_1 - ax_1^2 - bx_1 \quad (18)$$

The function of this parabola can be used to estimate the value of the minimum F_S and associated failure plane angle ($Beta_i$) using:

$$FS_{min} = \frac{4ac - b^2}{4a} \quad (19)$$

$$Beta_i = -\frac{b}{2a} \quad (20)$$

3.1.1 User Interface Development

Following the methods described above, the F_S module was developed using the programming language Python and the package Tkinter.

A user interface was developed for the F_S model (Figure 6). All the parameters shown in the GUI need to be input into the model, and parameters like gravitational acceleration constant, void ratio, and specific gravity are given a default value that can be changed as needed.

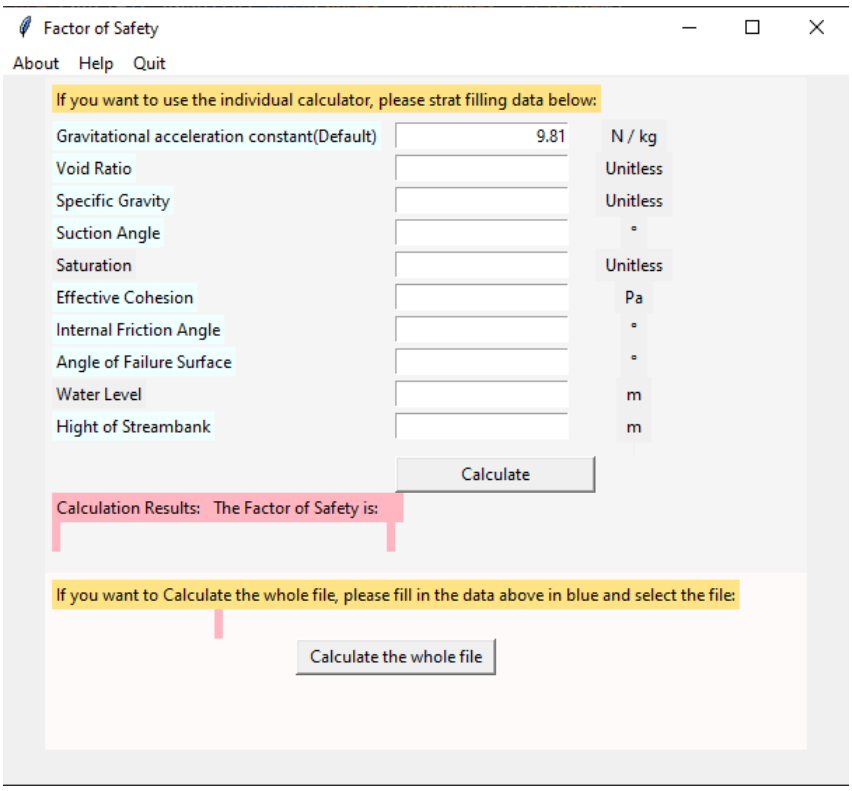

Figure 6: The user interface of the Streambank Stability Model

3.2 Model Verification

As there are no analytical solutions to verify the streambank stability model, we relied on results of similar models from peer-reviewed publications for verification. Further verification using a layer-refining approach will be pursued in future work.

In order to verify the model development as discussed, publications with similar F_S calculations and a complete listing of all the necessary input parameters are required. Unfortunately, most publications have not listed all the necessary data. Therefore, after comparing more than ten papers and their data, the model was verified using published results by Sutarto et al. (2014), who conducted similar, yet not identical, calculations at the Clear Creek watershed in Iowa, US. The results of this work and the input data are

summarized in Sutarto et al. (2014). The primary difference in the model formulation is that Sutarto et al. (2014) used horizontal layers, whereas the model developed here uses vertical slices. Despite this difference, we feel the results of Sutarto et al. (2014) were able to verify the new model. Their research selected 12 out of 48 different samples from the bank and focused on six study locations along the bank (Figure 7).

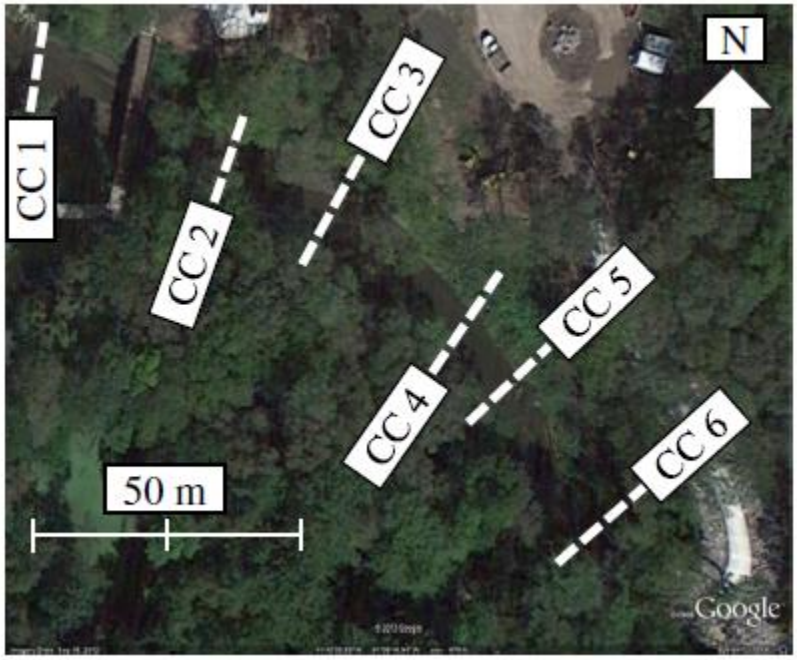

Figure 7 Study Spots in Clear Creek (Sutarto et al., 2014)

All the data and parameters used in the model verification from Sutarto et al. (2014) are provided in Table 2.

Table 2: Model Verification Data from Sutarto et al., (2014)

Test	Initial	Unit
Gravitational Acceleration Constant	9.81	N/kg
Void Ratio	0.54	-
Specific Gravity	3.28	-
Suction Angle	17.00	Degree
Saturation	1.00	-
Effective Cohesion	6000.00	Pa
Internal Friction Angle	34.88	Degree
The angle of Failure Surface	32.00	Degree
Water Level	2.50	m
Streambank Height	4.30	m

The factor of safety calculated using the model developed in this work was compared with the results shown in the literature, and the difference between them was calculated using the equation below:

$$Difference\% = \frac{|Model\ Value - Literature\ Value|}{Literature\ Value} \times 100\% \qquad (21)$$

A comparison between the literature data and model results is summarized in Table 3.

Table 3: Model Results vs. Literature Data (Sutarto et al., 2014)

Test	CC1	CC2	CC3	CC4	CC5	CC6	Average
Fs (new model)	2.99	2.97	2.96	2.95	2.95	2.96	2.96
Fs (Sutarto et al., 2014)	3.0	4.0	3.0	3.0	4.5	3.0	3.4
Difference (%)	0.33%	25.75%	1.33%	1.66%	34.44%	1.33%	12.9%

Table 3 shows that the difference between CC1, CC3, CC4, and CC6 is less than 2.00%, whereas results for CC2 and CC5 are much more significant. The differences in CC2 and

CC5 are likely due to the differences in model construction (horizontal vs. vertical layering) and heterogeneities in the geology and hydrology that were not specified in the paper. In the model developed here, streambanks are assumed to be homogeneous, but in natural conditions, there are many heterogeneities, even beyond those presented in Sutarto et al. (2014). These differences will contribute to uncertainty and errors between the two models. In addition, the data in the Sutarto et al. (2014) paper is separated into three horizontal layers: toe, midbank, and crest, but the model developed here was simplified into one horizontal layer in each vertical layer using averaged parameters. It is likely that conditions in CC1, CC3, CC4, and CC6 more closely reflect the average conditions, as opposed to those in CC2 and CC5. Given these assumptions, and the goal of this working being to develop a model that can provide preliminary estimates of streambank stability, we feel the model is adequately verified for this purpose.

Chapter 4.0: Model Demonstration

To demonstrate the use of the model framework developed here, we have applied it to a basin with an existing coupled HGS-OASIS model. The results presented here demonstrate the model's utility and do not provide robust predictions in this basin. Further work will provide a more robust application of this model to the site.

4.1 Site Description

The Lower Republican River Basin (LRRB) is located in southern Nebraska and northern Kansas (Figure 8). The entire Republican River basin covers approximately 65 billion square meters, with major rivers originating in northeastern Colorado (U.S. Department of the Interior, 2016). Approximately 31% of the basin is in Colorado, 30% is in Kansas, and 39% is in Nebraska. The dominant use of water in the basin is for agriculture, although water is also used for domestic, industrial, recreational, and wildlife purposes (U.S. Department of the Interior, 2016). Although aquifers underlie most of the basin, the basin is overallocated, and water resources are limited. As such, water management planning in the region is directly linked to economic health. Brookfield et al. (2015) coupled HGS and OASIS to simulate future water resources in the LRRB (Brookfield and Gnau, 2016), and Brookfield and Layzell (2019) expanded this model to include fluvial erosion to consider some components of sediment transport in the basin.

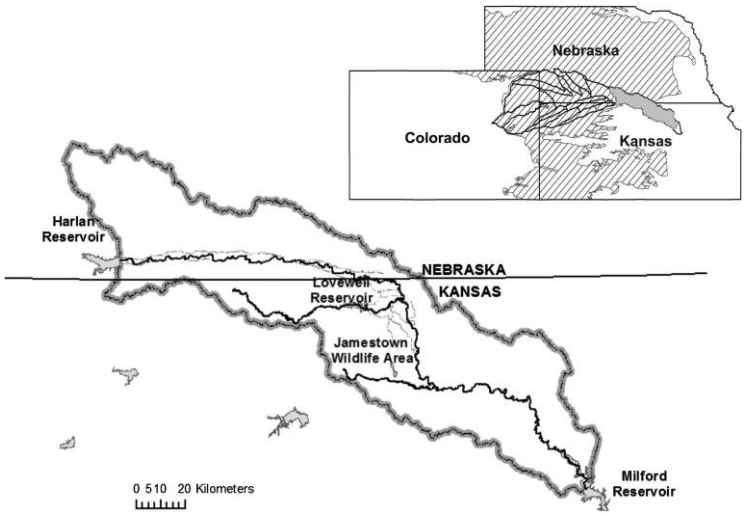

Figure 8: Lower Republican River Basin (Brookfield, 2016)

4.2 Model Parameterization

In this research, we demonstrate the new F_s model on the Lower Republican River Basin for two different hydrologic conditions resulting from extreme weather to simulate and indicate the effects of water management decisions on streambank stability. Results from the coupled HGS-OASIS model were selected for two points in time to reflect wet and dry hydrologic conditions. These times were selected based on regional climate conditions, as indicated by the National Integrated Drought Information System (Figure 9) (Drought.gov, 2022).

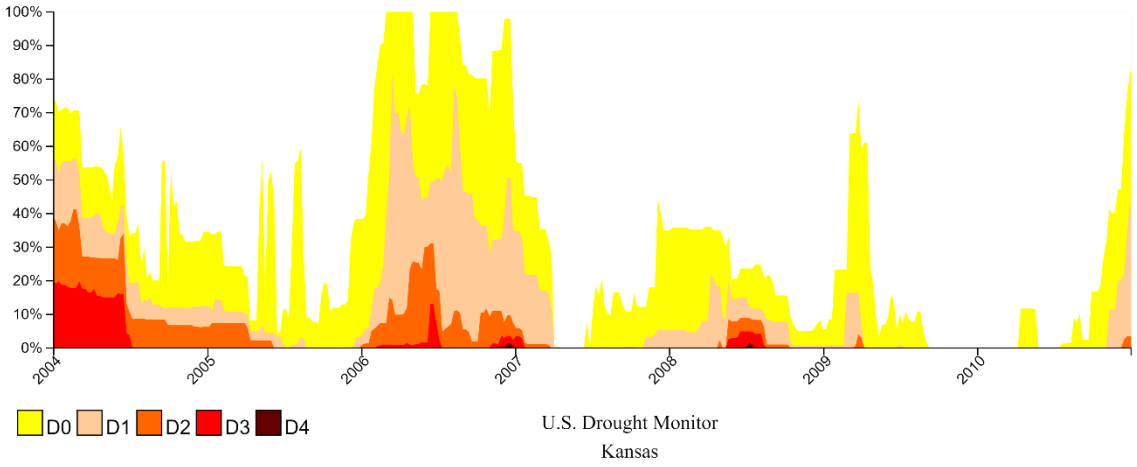

Figure 9 National Integrated Drought Information System (2022)

As can be observed in Figure 9, a severe drought occurred in July 2005, which typically causes decreases in surface water and groundwater resources and increases in water demand from reservoirs. In addition, the drought conditions were prolonged prior to July 2005, reducing the influence of antecedent wetness on the hydrologic conditions. Therefore, July 2005 was selected as the dry scenario. Conversely, the time leading up to July 2010 was one of the few recent prolonged periods where no drought was observed in this basin, and therefore July 2010 will be selected as the wet scenario. During a typical wet scenario, groundwater and surface water resources increase, and water demand from reservoirs decreases.

4.2.1 Input Data

Parameters like void ratio, bank height, and specific gravity were measured directly in the field by Dr. Tony Layzell of the Kansas Geological Survey (KGS) as part of this work.

While these parameters did vary with different sites along the basin, we are using average parameters throughout the model site, as the purpose of this demonstration is to show how the model can be applied and the results it can present. The internal friction angle, cohesion, and suction angle were also measured in the field by Dr. Layzell using the borehole shear test (BST), as shown in Figure 10 (HANDY, 2022). Values measured in the field will be averaged for this model demonstration.

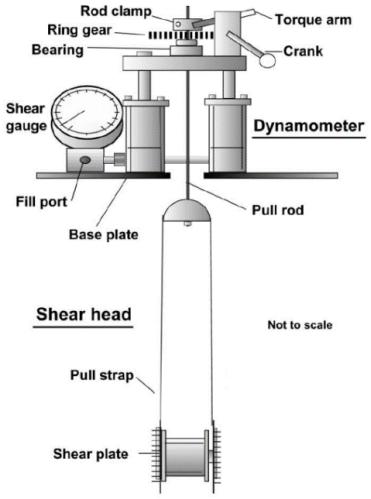

Figure 10: Borehole Shear Test (HANDY, 2022)

During BST, normal stress is applied (commonly using gas) to the shear plate on a streambank parcel to let the bank material consolidate. Then vertical shear is applied to it to measure the failure shear strength. After repeating several times with different normal stresses, a plot is generated with all the points with an x-axis of normal strength and a y-axis of shear strength. Figure 11 is an example of a classic plot for BST measurements, where the line crosses the y-axis is the efficient cohesion (c') in kPa. The slope of that trend line is the internal friction angle (Φ') (Lazyell, 2021).

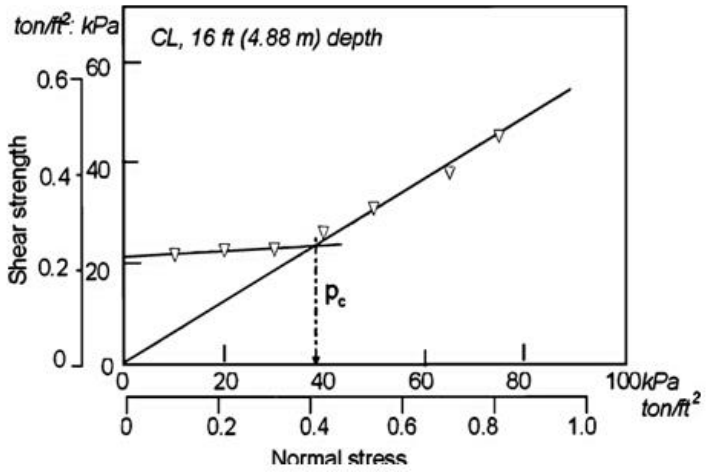

Figure 11: Classic Plot for BST Measurements (HANDY, 2022)

The suction angle is the angle of the line in a plot of matric suction and shear strength under constant normal stress (Elsharief & Abdulaziz, 2015). The data used in this model demonstration were collected from the study field in LRRB, Kansas, and analyzed by Dr. Layzell at the KGS. The average values of this data, as input to the stability model, are summarized in Table 4.

Table 4: Data collected in Kansas (Layzell, 2021)

Parameters	Values	Unit
Gravitational Acceleration Constant	9.81	N/kg
Void Ratio	0.40	-
Specific Gravity	2.75	-
Suction Angle	17.00	Degree
Effective Cohesion	7200.00	Pa
Internal Friction Angle	32.60	Degree
Angle of Failure Surface	56.00	Degree
Streambank Height	2.70	m

As previously mentioned, this model can use an output file from HGS to characterize the hydrologic conditions. In this demonstration, results from the coupled HGS and OASIS model for the LRRB are used for July 2005 and 2010 (Brookfield et al., 2017). The main output files used in this research are those for overland flow (*.olf), which provides data on the depth of the surface water, and the for porous media (*.pm), which provides data on the groundwater levels and pore pressures.

After running the F_s model, the output file is displayed in ArcGIS using the associated nodal coordinates from the HGS model grid. This allows for the generation of a map that demonstrates the spatial variability of F_S across the basin.

4.3 Model Results

Previous chapters discussed how groundwater and surface water levels, and therefore different water management decisions, would affect streambank stability. July 2010 is used for the wet scenario to study the effects of high water levels and fast flow, and July 2005 is used for the dry scenario to study the effect of low water levels and low flow on streambank stability. The intention of this model demonstration is to show how the model can be used to assess streambank stability. Due to the simplifications of both the method and the data used in this model, particularly the averaged field parameters, the uncertainty of this model is significant, and the results are not appropriate for assessing streambank stability in the LRRB. This demonstration will illustrate how different

hydrologic conditions, driven by water management decisions, can affect streambank stability.

4.3.1 Wet Scenario

As previously described, July 2010 was selected as the wet scenario for this model demonstration. Figure 12 shows the streambanks' failure map in the LRRB, where the red dots indicate streambank failures at that node. 92 nodal locations in that area were labeled as unstable or would be unstable soon (F_S <=1). Most nodes are located along the main river of the Republican River. Figure 12 shows that all the failure areas are evenly distributed along the stream, although fewer failure areas are in the upstream region of the basin.

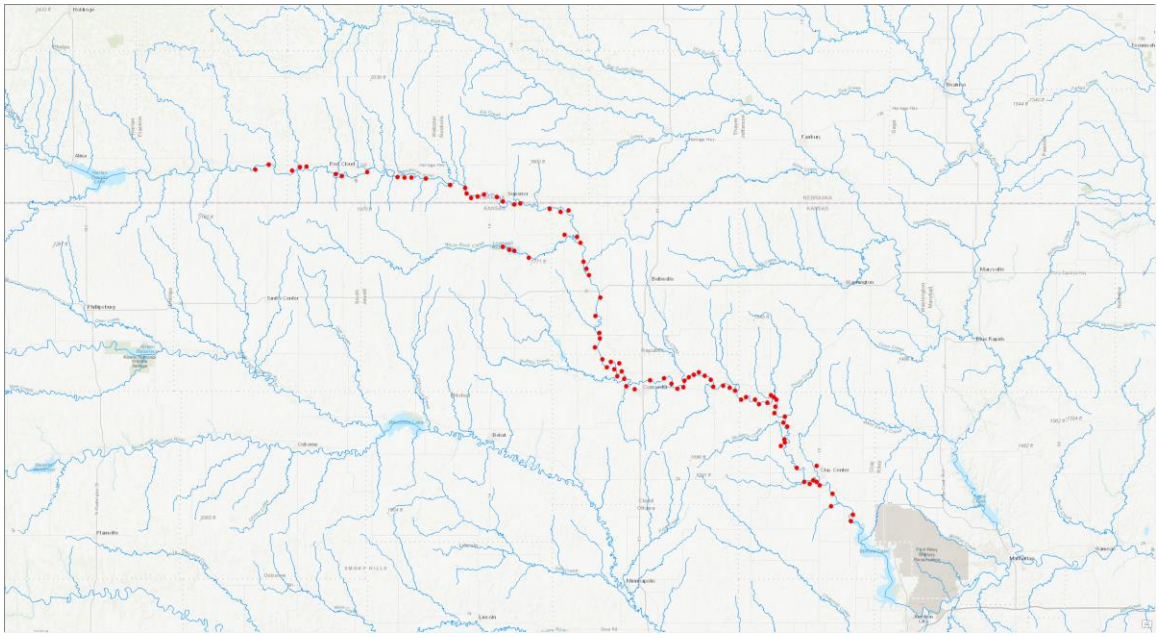

Figure 12: Streambank Instability Map for wet scenario

For the approximate 10000 nodes in the LRRB, the average value of the factor of safety for the whole basin is 2.28, with a minimum value of 0.01 and a maximum value of 3.34. Furthermore, all the failure areas have an average factor of safety value of 0.37. If we restrict the analysis to the 737 nodes along the main rivers of LRRB, 83 nodes are labeled as unsafe, with a lower average factor of safety of 2.03 and a lower maximum value of these nodes is 2.34. The minimum value remains the same at 0.01. Figure 13 shows the percentage of safe, unsafe, and soon-to-be unsafe areas. Although the unsafe proportion is relatively small in the figure, the potential for streambank failure is widespread and significant (Figure 13).

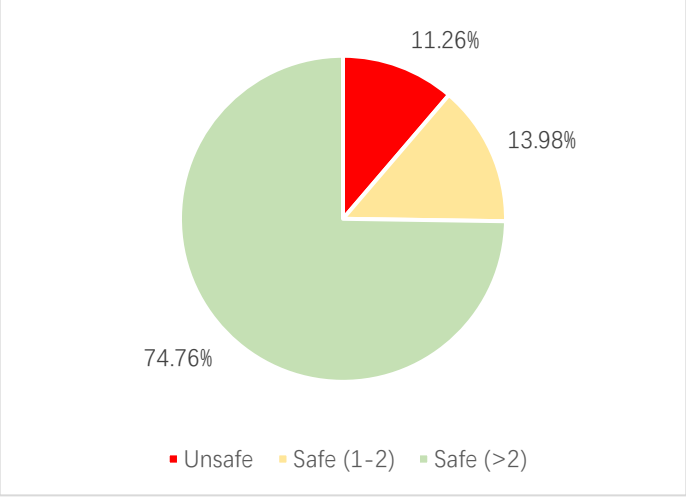

Figure 13: Percentage of Safe Areas and Unsafe Areas in wet scenario

4.3.2 Dry Scenario

As described previously, July 2005 was selected to represent a dry scenario for this demonstration. Figure 14 is the map of failure at LRRB in July 2005. 84 nodal locations in that area were labeled as unstable or would be unstable soon (F_S <=1).

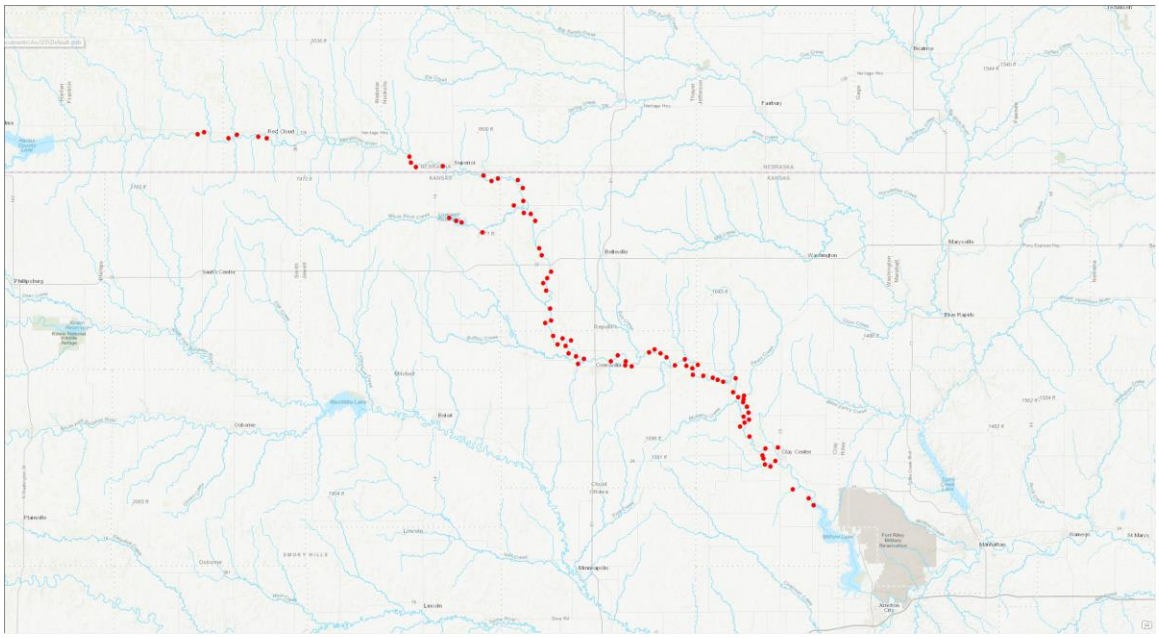

Figure 14: Streambank Instability Map for dry scenario

The average factor of safety in this scenario is 2.29, higher than in July 2010, which means, on average, the streambanks in the basin were more stable in July 2010. The minimum value of the factor of safety is 0.01, while the maximum value is 3.34. In addition, the average factor of safety value in unsafe areas is 0.37, which is more stable than the unsafe areas identified in the July 2010 simulations. Compared with July 2010, the number of unsafe nodes along the main river decreased significantly in July 2005.

Only 70 nodes were marked as unsafe out of 737 points along the main river; the average, maximum and minimum values of all these nodes are 2.34, 2.07, and 0.01, respectively. Figure 15 shows the percentage of safe, unsafe, and soon-to-be unsafe areas. Compared with the wet scenario, there were fewer unsafe areas in the dry scenario.

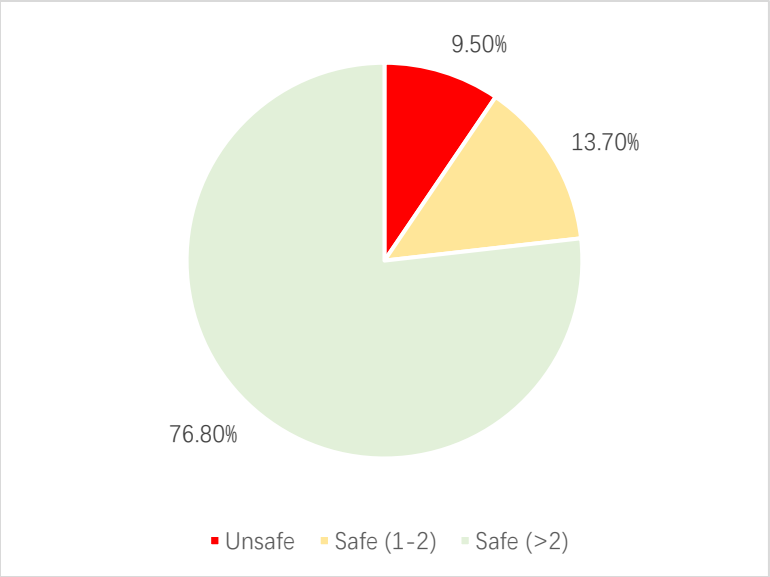

Figure 15: Percentage of Safe Area and Unsafe Area in dry scenario

4.4 Discussion

Scientific planning and management of water resources, including water supply and demand management, distribution management, and extreme weather management, are critical to this basin's economic, ecosystem, and human health. As seen in the previous section, the stability of the streambank is not the same under dry and wet conditions when both hydrologic conditions and water management strategies are significantly different. In general, in dry conditions, the overall stability of streambanks is higher than in wet scenarios, likely due to decreased soil loading due to low soil moisture, which is reflected

in the high average factor of safety. In addition, the factor of safety in unstable areas is also higher in dry conditions than in wet conditions. Under different weather conditions, water management decisions are also different; for example, in extremely dry conditions, reservoirs will store as much water as possible to meet the water supply to irrigators. Therefore, the groundwater level in that area would be lower than average, but the surface water level might be relatively high due to releasing water. This would result in higher hydrostatic forces from the surface water, combined with lower saturation of the streambank soil, pore water pressure, and soil unit weight, leading to higher overall streambank stability. In wet conditions, due to sufficient water availability, to prevent reducing the impact of downstream floods, the reservoir will maintain safe downstream flows yet retain sufficient water for future releases. Due to the combination of reservoir releases and natural flow from precipitation, surface water levels during these times will be high. Yet, due to increased infiltration and precipitation, the soil saturation of streambanks will also be high, increasing the pore water pressure and the soil unit weight, which can increase the risk of bank instability.

Chapter 5.0: Conclusions and Recommendations

Streambank stability is affected by many factors and is significantly affected by human activities such as the construction of large reservoirs and river routing projects. Though these water-related infrastructure and water management decisions are essential to the safety of the downstream regions and the stability of water resources, several water management decisions may negatively affect streambank stability. In this research, the effects of water management on streambank stability were studied through the development of a new model to estimate the F_S using results from HGS simulations. This model was verified using previously published research that applied a similar F_S method to field conditions and was demonstrated with a wet and dry scenario in the LRRB.

In applying the verified model to the LRRB, it is evident that water management decisions do have an impact on the stability of streambanks, mainly due to three aspects: 1) the influence on the pore water pressure, which is the ability of streambank soils to maintain their structure; 2) the impact of the weight of the streambank soil as a heavier soil parcel will make streambanks less stable and increase the risks of failure, and 3) the impact of stream water levels the forces which can maintain streambank stability. While water resources management under extreme weather can reduce the risk of floods and provide water to downstream users as needed, it can also have an adverse effect on the

stability of streambanks through the rapid water increases and decreases during and after reservoir release events.

The approach and model used in this research greatly simplify many features of natural streambanks and streambank stability. This research intended to provide a tool for preliminary assessment of streambank stability under hydrologic conditions driven by water management decisions. The model and the application demonstrated here include many assumptions and thus have significant uncertainty. While this work has shown that the existing framework can provide preliminary assessments of streambank stability and differentiation between different hydrologic conditions, further work is needed to improve the model and its performance. This will include further verification using layer-refining to ensure spatial stability, modifications to allow for heterogeneous streambank materials, and to assess the implications of assuming hydrostatic pressure. Despite these considerations, the model developed in this work does provide a new tool for water management decision-making of both water quantity and streambank stability, which has the potential to contribute to more efficient water management decisions.

References

Admiraal, D. M. (2007). Streambank stabilization using traditional and bioengineering methods: A literature review.

An, Lu, W., & Yan, X. (2018). A surrogate-based simulation–optimization approach application to parameters' identification for the HydroGeoSphere model. Environmental Earth Sciences, 77(17), 1–8. https://doi.org/10.1007/s12665-018-7806-7

Asselt, M. B. A. van. (2001). Integrated water management strategies for the Rhine and Meuse basins in a changing environment. Bilthoven, The Netherlands: National Institute of Public Health and the Environment.

Bankhead, N., Entrix, C., Simon, A., & Thomas, R. E. (2013). Experiments, model development and bank stability simulations to assess bank erosion rates and potential mitigation strategies. Report to the USDA Forest Service, Pacific Southwest Research Station, 1731.

Basheer, & Elagib, N. A. (2018). Sensitivity of Water-Energy Nexus to dam operation: A Water-Energy Productivity concept. The Science of the Total Environment, 616-617, 918–926. https://doi.org/10.1016/j.scitotenv.2017.10.228

Beegum, S., Šimůnek, J., Szymkiewicz, A., Sudheer, K., & Nambi, I. (2018). Updating the Coupling Algorithm between HYDRUS and MODFLOW in the HYDRUS

Package for MODFLOW. Vadose Zone Journal, 17(1), 1–8. https://doi.org/10.2136/vzj2018.02.0034

Benjamin N O Kuffour, Nicholas B Engdahl, Carol S Woodward, Laura E Condon, Stefan Kollet, & Reed M Maxwell. (2020). Simulating coupled surface–subsurface flows with ParFlow v3.5.0: capabilities, applications, and ongoing development of an open-source, massively parallel, integrated hydrologic model. Geoscientific Model Development, 13(3), 1373–1397. https://doi.org/10.5194/gmd-13-1373-2020

Borg, D. (2014). Assessment of Streambank Stability-A Case Study. In Geo-Congress 2014 (pp. 1007–1016). https://doi.org/10.1061/9780784413272.098

Brookfield, A., Gnau, C., & Wilson, B. (2017). Incorporating Surface Water Operations in an Integrated Hydrologic Model: Model Development and Application to the Lower Republican River Basin, United States. Journal of Hydrologic Engineering, 22(4), 4016065–. https://doi.org/10.1061/(ASCE)HE.1943-5584.0001486

Brookfield, A., & Layzell, A. (2019). Simulating the Effects of Reservoir Management Strategies on Fluvial Erosion. Water Resources Management, 33(15), 4983–4995. https://doi.org/10.1007/s11269-019-02380-y

Brunner, P., & Simmons, C. (2012). HydroGeoSphere: A Fully Integrated, Physically Based Hydrological Model. Ground Water, 50(2), 170–176. https://doi.org/10.1111/j.1745-6584.2011.00882.x

Casagli, R. (1999). Pore water pressure and streambank stability: results from a monitoring site on the Sieve River, Italy. Earth Surface Processes and Landforms, 24(12), 1095–1114. https://doi.org/10.1002/(SICI)1096-9837(199911)24:12<1095::AID-ESP37>3.0.CO;2-F

Center for advanced Decision Support for Water and Environmental Systems (2019). Solution Approaches. RiverWare Technical Documentation Version 8.0. https://www.riverware.org/PDF/RiverWare/documentation/SolutionApproaches.pdf

Chu-Agor, M., Wilson, G., & Fox, G. (2008). Numerical Modeling of Bank Instability by Seepage Erosion Undercutting of Layered Streambanks. Journal of Hydrologic Engineering, 13(12), 1133–1145. https://doi.org/10.1061/(ASCE)1084-0699(2008)13:12(1133)

Condon, M. (2013). Implementation of a linear optimization water allocation algorithm into a fully integrated physical hydrology model. Advances in Water Resources, 60, 135–147. https://doi.org/10.1016/j.advwatres.2013.07.012

Crowder, D. (2007). The accuracy of sediment loads when log-transformation produces non-linear sediment load–discharge relationships. Journal of Hydrology (Amsterdam), 336(3), 250–268. https://doi.org/10.1016/j.jhydrol.2006.12.024

Diersch. (2014). FEFLOW : finite element modeling of flow, mass and heat transport in porous and fractured media. Springer.

Donohue, Ian & Molinos, Jorge. (2009). Impacts of Increased Sediment Loads on the Ecology of Lakes. Biological Reviews of the Cambridge Philosophical Society. 84. 517-31. 10.1111/j.1469-185X.2009.00081.x.\

Drought.gov. (2022). National Integrated Drought Information System. From Website: https://www.drought.gov/states/kansas

Duan, G., Shu, A., Rubinato, M., Wang, S., & Zhu, F. (2018). Collapsing Mechanisms of the Typical Cohesive Streambank along the Ningxia–Inner Mongolia Catchment. Water (Basel), 10(9), 1272–. https://doi.org/10.3390/w10091272

Elsharief1 A.M. & Abdulaziz O.A. (2015). Effects of Matric Suction on the Shear Strength of Highly Plastic Compacted Clay

Erskine, W. D. (2005). Sediment Load Measurements. Water Encyclopedia. John Wiley & Sons, Inc. p. 397.

Fatiha Choukri, Damien Raclot, Mustapha Naimi, Mohamed Chikhaoui, João Pedro Nunes, Frédéric Huard, Cécile Hérivaux, Mohamed Sabir, & Yannick Pépin. (2020). Distinct and combined impacts of climate and land use scenarios on water availability and sediment loads for a water supply reservoir in northern Morocco. International Soil and Water Conservation Research, 8(2), 141–153.

Fox, G., Midgley, T., & Heeren, D. (2011). Evaluation of the Bank Stability and Toe Erosion Model (BSTEM) for Predicting Lateral Streambank Retreat on Ozark

Streams. World Environmental and Water Resources Congress 2011, 1991–2000. https://doi.org/10.1061/41173(414)209

Fredlund, Meng, S., Zyvolosk, G. A., Stauffer, P. H., & Orr, S. (2018). Benchmarking of FEHM Control Volume Finite Element Solver. In Proceedings of the 8th International Congress on Environmental Geotechnics Volume 1 (pp. 528–535). Springer Singapore. https://doi.org/10.1007/978-981-13-2221-1_57

Greer, C. (1976). Chinese water management strategies in the Yellow River basin. University of Washington, Seattle.

Greenfield, M. (2015). A tiered assessment framework to evaluate human health risk of contaminated sediment: Assessment Framework for Human Health Risk of Sediment. Integrated Environmental Assessment and Management, 11(3), 459–473. https://doi.org/10.1002/ieam.1610

HANDY GeoTechnical Instruments (2022). From Website: https://handygeotech.com/borehole-shear/

Harbaugh, A. W. (2005). MODFLOW-2005, the US Geological Survey modular groundwater model: the groundwater flow process (pp. 6-A16). Reston, VA: US Department of the Interior, US Geological Survey.

Hydrologics. (2009). "OASIS with OCL, model version 3.10.8, GUI version 4.6.16." Columbia, MD.

Hydrologics. (2009). User Manual for OASIS WITH OCL

Kim, Chung, I. M., Won, Y. S., & Arnold, J. G. (2008). Development and application of the integrated SWAT–MODFLOW model. Journal of Hydrology (Amsterdam), 356(1-2), 1–16. https://doi.org/10.1016/j.jhydrol.2008.02.024

Klavon, K., Fox, G., Guertault, L., Langendoen, E., Enlow, H., Miller, R., & Khanal, A. (2017). Evaluating a process-based model for use in streambank stabilization: insights on the Bank Stability and Toe Erosion Model (BSTEM). Earth Surface Processes and Landforms, 42(1), 191–213. https://doi.org/10.1002/esp.4073

Kollet, S., & Maxwell, R. (2006). Integrated surface–groundwater flow modelling: A free-surface overland flow boundary condition in a parallel groundwater flow model. Advances in Water Resources, 29(7), 945–958. https://doi.org/10.1016/j.advwatres.2005.08.006

Lalehzari, R., Boroomand Nasab, S., Moazed, H., Haghighi, A., & Yaghoobzadeh, M. (2020). SIMULATION–OPTIMIZATION MODELLING FOR WATER RESOURCES MANAGEMENT USING NSGAII-OIP AND MODFLOW. Irrigation and Drainage, 69(3), 317–332. https://doi.org/10.1002/ird.2424

Langendoen, E. J. (2000). Concepts: Conservational channel evolution and pollutant transport system. USDA-ARS National Sedimentation Laboratory.

Langendoen, E. J., Zegeye, A., Steenhuis, T., Ayele, G., Tilahun, S., & Ayana, E. (2014). Using computer models to design gully erosion control structures for humid northern

Ethiopia. In ICHE 2014. Proceedings of the 11th International Conference on Hydroscience & Engineering (pp. 1137-1146).

Langevin, C.D., Hughes, J.D., Banta, E.R., Niswonger, R.G., Panday, Sorab, and Provost, A.M., 2017, Documentation for the MODFLOW 6 Groundwater Flow Model: U.S. Geological Survey Techniques and Methods, book 6, chap. A55, 197 p., https://doi.org/10.3133/tm6A55.

Li, Q., Unger, A., Sudicky, E., Kassenaar, D., Wexler, E., & Shikaze, S. (2008). Simulating the multi-seasonal response of a large-scale watershed with a 3D physically-based hydrologic model. Journal of Hydrology (Amsterdam), 357(3), 317–336. https://doi.org/10.1016/j.jhydrol.2008.05.024

Markstrom, Steven & Regan, Robert & Niswonger, R. & Prudic, D. & Barlow, Paul. (2016). GSFLOW: coupled groundwater and surface-water flow model. 10.5066/F7WW7FS0.

Maxwell, R., Condon, L., & Kollet, S. (2015). A high-resolution simulation of groundwater and surface water over most of the continental US with the integrated hydrologic model ParFlow v3. Geoscientific Model Development, 8(3), 923–937. https://doi.org/10.5194/gmd-8-923-2015

McKinney, D. C. (2004). TECHNICAL REPORT INTERNATIONAL SURVEY OF DECISION SUPPORT SYSTEMS FOR INTEGRATED WATER MANAGEMENT. Support to Enhance Privatization, Investment, and

Competitiveness in the Water Sector of the Romanian Economy (SEPIC) IRG PROJECT, (1673-000).

Midgley, F. (2012). Evaluation of the bank stability and toe erosion model (BSTEM) for predicting lateral retreat on composite streambanks. Geomorphology (Amsterdam, Netherlands), 145-146, 107–114. https://doi.org/10.1016/j.geomorph.2011.12.044

Mohammed-Ali, W., Mendoza, C., & Holmes, R. (2019). Streambank stability assessment during hydro-peak flow events: the lower Osage River case (Missouri, USA). International Journal of River Basin Management, ahead-of-print(ahead-of-print), 1–9. https://doi.org/10.1080/15715124.2020.1738446

National Integrated Drought Information System (2022). From Website: https://www.drought.gov/historical-information?state=kansas&dataset=0&selectedDateUSDM=20021231&dateRangeUSDM=2002-2004

Okeke, C., Ede, A., & Kogure, T. (2019). Monitoring of streambank stability and seepage undercutting mechanisms on the Iju (Atuwara) River, Southwest Nigeria. IOP Conference Series. Materials Science and Engineering, 640(1), 12105–. https://doi.org/10.1088/1757-899X/640/1/012105

Osman, A., & Thorne, C. (1988). Streambank Stability Analysis. I: Theory. Journal of Hydraulic Engineering (New York, N.Y.), 114(2), 134–150. https://doi.org/10.1061/(ASCE)0733-9429(1988)114:2(134)

Preece, E., Hobbs, W., Hardy, F., O'Garro, L., Frame, E., & Sweeney, F. (2021). Prevalence and persistence of microcystin in shoreline lake sediments and porewater, and associated potential for human health risk. Chemosphere (Oxford), 272, 129581–129581. https://doi.org/10.1016/j.chemosphere.2021.129581

Qiu, J., Yang, Q., Zhang, X., Huang, M., Adam, J., & Malek, K. (2019). Implications of water management representations for watershed hydrologic modelling in the Yakima River basin. Hydrology and Earth System Sciences, 23(1), 35–49. https://doi.org/10.5194/hess-23-35-2019

Shadi Moqbel, & Wa'il Abu-El-Sha'r. (2018). Modeling Groundwater Flow and Solute Transport at Azraq Basin Using ParFlow and Slim - Fast. Jordan Journal of Civil Engineering, 12(2).

Simon, A., Curini, A., Darby, S., & Langendoen, E. (2000). Bank and near-bank processes in an incised channel. Geomorphology (Amsterdam, Netherlands), 35(3), 193–217. https://doi.org/10.1016/S0169-555X(00)00036-2

Surfleet, & Tullos, D. (2013). Uncertainty in hydrologic modelling for estimating hydrologic response due to climate change (Santiam River, Oregon). Hydrological Processes, 27(25), 3560–3576. https://doi.org/10.1002/hyp.9485

Sutarto, Papanicolaou, A. N. (Thanos), Wilson, C. G., & Langendoen, E. J. (2014). Stability Analysis of Semicohesive Streambanks with CONCEPTS: Coupling Field and Laboratory Investigations to Quantify the Onset of Fluvial Erosion and Mass

Failure. *Journal of Hydraulic Engineering (New York, N.Y.)*, *140*(9). https://doi.org/10.1061/(ASCE)HY.1943-7900.0000899

Taie Semiromi, M., & Koch, M. (2019). Analysis of Spatio-temporal variability of surface–groundwater interactions in the Gharehsoo river basin, Iran, using a coupled SWAT-MODFLOW model. Environmental Earth Sciences, 78(6), 1–21. https://doi.org/10.1007/s12665-019-8206-3

Therrien R, McLaren RG, Sudicky EA, Panday SM (2010) HydroGeoSphere: a three-dimensional numerical model describing fully-integrated subsurface and surface flow and solute transport. Groundwater Simulations Group, University of Waterloo, Waterloo

Therrien, R., McLaren, R. G., Sudicky, E. A., and Panday, S. M. (2007). "HydroGeoSphere: A three-dimensional numerical model describing fully-integrated subsurface and surface flow and solute transport." Groundwater Simulations Group, Univ. of Waterloo, Waterloo, ON, Canada.

US Army Corps of Engineers (2015). HEC-RAS USDA-ARS Bank Stability & Toe Erosi on Model (BSTEM), Technical Reference & User's Manual. From Website: https:// www.hec.usace.army.mil/confluence/rasdocs/rassed1d/1d-sediment-transport-technic al-reference-manual/bstem-technical-reference-manual/steps-in-a-bank-failure-analys is.

U.S. Department of the Interior (2016). FINAL FULL REPORT: Republican River Basin Study. https://www.usbr.gov/watersmart/bsp/docs/finalreport/republican/republican-river-basin-study-final-report.pdf

Steven L. Markstrom, Richard G. Niswonger, R. Steven Regan, David E. Prudic, and Pau l M. Barlow (2005). GSFLOW—Coupled Ground-Water and Surface-Water Flow M odel Based on the Integration of the Precipitation-Runoff Modeling System (PRMS) and the Modular Ground-Water Flow Model (MODFLOW-2005)

Valerio, A., Rajaram, H., & Zagona, E. (2010). Incorporating Groundwater-Surface Water Interaction into River Management Models. Ground Water, 48(5), 661–673. https://doi.org/10.1111/j.1745-6584.2010.00702.x

Yang, Z. (2007). Influence of the Three Gorges Dam on downstream delivery of sediment and its environmental implications, Yangtze River. Geophysical Research Letters, 34(10), L10401–n/a. https://doi.org/10.1029/2007GL029472

Zagona, Fulp, T. J., Shane, R., Magee, T., & Goranflo, H. M. (2001). RIVERWARE: A GENERALIZED TOOL FOR COMPLEX RESERVOIR SYSTEM MODELING1. Journal of the American Water Resources Association, 37(4), 913–929. https://doi.org/10.1111/j.1752-1688.2001.tb05522.x

Zhang, L. (2008). Recent changes of water discharge and sediment load in the Zhujiang (Pearl River) Basin, China. Global and Planetary Change, 60(3), 365–380. https://doi.org/10.1016/j.gloplacha.2007.04.003

Appendices

Appendix A: Simplified Method

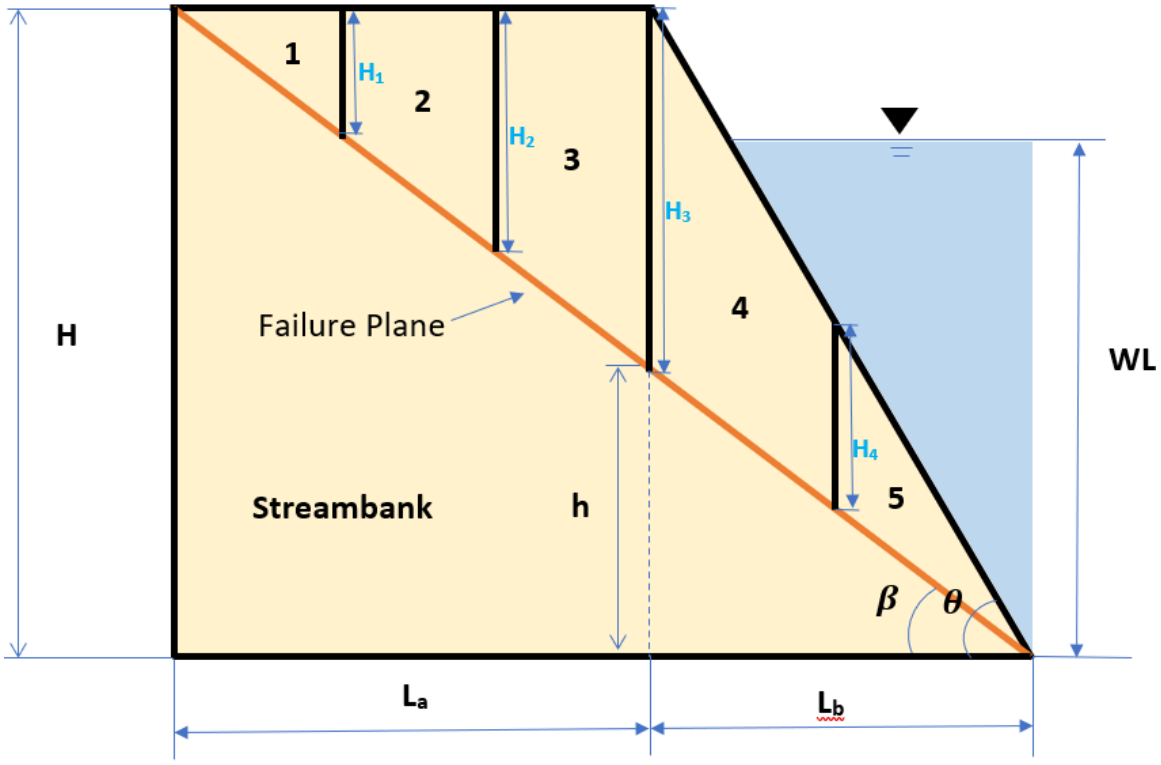

Figure 16: Simplified Method For Each Slide

H is the height of the streambank, and WL is the Water Level in that area. Thus, these two values can be measured directly from the field. The length of the streambank L_b can be calculated as:

$$L_b = \frac{H}{\tan(\theta)}$$

$$or\ L_b = \frac{h}{\tan(\beta)}$$

Therefore, h can be calculated as:

$$h = \frac{H \tan(\beta)}{\tan(\theta)}$$

Then H_3 is:

$$H_3 = H - h$$

$$H_1 = \frac{1}{3} H_3 = \frac{1}{3} (H - h)$$

$$H_2 = \frac{2}{3} H_3 = \frac{2}{3} (H - h)$$

$$H_4 = \frac{1}{2} H_3 = \frac{1}{2} (H - h)$$

Thus, L_a can be determined as:

$$L_a = \frac{H_3}{\tan(\beta)} = \frac{(H - h)}{\tan(\beta)}$$

So:

$$A_1 = \frac{1}{2} \times H_1 \times \frac{1}{3} L_a = \frac{1}{18} \frac{(H - h)^2}{\tan(\beta)}$$

$$A_2 = \frac{1}{2} \times (H_1 + H_2) \times \frac{1}{3} L_a = \frac{3}{18} \frac{(H - h)^2}{\tan(\beta)}$$

$$A_3 = \frac{1}{2} \times (H_2 + H_3) \times \frac{1}{3} L_a = \frac{5}{18} \frac{(H - h)^2}{\tan(\beta)}$$

$$A_4 = \frac{1}{2} \times (H_3 + H_4) \times \frac{1}{2} L_b = \frac{3}{8} \frac{H(H - h)}{\tan(\theta)}$$

$$A_5 = \frac{1}{2} \times H_4 \times \frac{1}{2} L_b = \frac{1}{8} \frac{H(H - h)}{\tan(\theta)}$$

Therefore, assume the width of the streambank is W_a, the volume of each layer can be determined as:

$$V_1 = A_1 \times W_a = \frac{1}{18} \frac{(H - h)^2}{\tan(\beta)} W_a$$

$$V_2 = A_2 \times W_a = \frac{3}{18} \frac{(H - h)^2}{\tan(\beta)} W_a$$

$$V_3 = A_3 \times W_a = \frac{5}{18} \frac{(H - h)^2}{\tan(\beta)} W_a$$

$$V_4 = A_4 \times W_a = \frac{3}{8} \frac{H(H - h)}{\tan(\theta)} W_a$$

$$V_5 = \ A_5 \times W_a = \frac{1}{8}\frac{H(H-h)}{\tan(\theta)}W_a$$

All the values are summarized in Table 1.

Appendix B: Streambank Stability Model Codes

```
# import

#import heartrate; heartrate.trace(browser = True)

from tkinter import *

from tkinter import messagebox as dialog

from tkinter import filedialog

from tkinter.filedialog import askopenfile

import math

import re

import xlwt

import xlrd


#window size

HEIGHT = 500

WIDTH = 600


window = Tk()


#Define Input value

class Calculator:
```

```
def __init__(self):

    window.title("Factor of Safety")



    self.g = StringVar()

    self.void_ratio = StringVar()

    self.specific_gravity = StringVar()

    self.Yb = StringVar()

    self.Saturation = StringVar()

    self.Effective_cohension = StringVar()

    self.Y = StringVar()

    self.T = StringVar()

    self.WL = StringVar()

    self.H = StringVar()

    self.Fs = StringVar()

    self.Result = StringVar()

    self.Notice = StringVar()

    self.Beta_result =  StringVar()

    self.Beta_notice =StringVar()
```

```
# Default Values

self.void_ratio.set("0.4")

self.g.set('9.81')

self.specific_gravity.set('3')

#self.Yb.set('17')

#self.Effective_cohension.set('4500')

#self.Y.set('29.9')

#self.T.set('56')

#self.H.set('2.7')


canvas = Canvas(window, height=HEIGHT, width=WIDTH)

canvas.pack()


Intro1 = Frame(window, bg='#f5f5f5', bd=5)

Intro1.place(relx=0.5, rely=0.00, relwidth=0.9, relheight=0.05, anchor='n')

frame = Frame(window, bg='#f5f5f5', bd=5)

frame.place(relx=0.5, rely=0.05, relwidth=0.9, relheight=0.65, anchor='n')

Lower_frame = Frame(window, bg='#fffafa', bd=5)

Lower_frame.place(relx=0.5, rely=0.7, relwidth=0.9, relheight=0.25, anchor='n')
```

```
#frame = Frame(window)

#frame.pack(padx=25, pady=20)


Label(Intro1, text="If you want to use the individual calculator, please strat filling data below:", bg='#ffe384').grid(row=0, column=1, columnspan=3)

Label(frame, text="Gravitational acceleration constant(Default)",bg='#F0FFFF').grid(row=1, column=1, columnspan=3, sticky=W)

Label(frame, text="Void Ratio",bg='#F0FFFF').grid(row=2, column=1, columnspan=3, sticky=W)

Label(frame, text="Specific Gravity",bg='#F0FFFF').grid(row=3, column=1, columnspan=3, sticky=W)

Label(frame, text="Suction Angle",bg='#F0FFFF').grid(row=4, column=1, columnspan=3, sticky=W)

Label(frame, text="Saturation").grid(row=5, column=1, columnspan=3, sticky=W)

Label(frame, text="Effective Cohesion",bg='#F0FFFF').grid(row=6, column=1, columnspan=3, sticky=W)

Label(frame, text="Internal Friction Angle",bg='#F0FFFF').grid(row=7, column=1, columnspan=3, sticky=W)

Label(frame, text="Angle of Failure Surface",bg='#F0FFFF').grid(row=8, column=1, columnspan=3, sticky=W)
```

```
Label(frame, text="Water Level",bg='#F0FFFF').grid(row=9, column=1,
columnspan=3, sticky=W)
Label(frame, text="Hight of Streambank").grid(row=10, column=1, columnspan=3,
sticky=W)
Label(Lower_frame, text="If you want to Calculate the whole file, please fill in the
data above in blue and select the file:",bg='#ffe384').grid(row=0, column=1,
columnspan=3)
#Input Values
Entry(frame, justify=RIGHT, textvariable=self.g).grid(row=1, column=3, sticky=W)
Entry(frame, justify=RIGHT, textvariable=self.void_ratio).grid(row=2, column=3,
sticky=W)
Entry(frame, justify=RIGHT, textvariable=self.specific_gravity).grid(row=3,
column=3, sticky=W)
Entry(frame, justify=RIGHT, textvariable=self.Yb).grid(row=4, column=3,
sticky=W)
Entry(frame, justify=RIGHT, textvariable=self.Saturation).grid(row=5, column=3,
sticky=W)
Entry(frame, justify=RIGHT, textvariable=self.Effective_cohension).grid(row=6,
column=3, sticky=W)
```

```
        Entry(frame, justify=RIGHT, textvariable=self.Y).grid(row=7, column=3,
sticky=W)
        Entry(frame, justify=RIGHT, textvariable=self.T).grid(row=8, column=3,
sticky=W)
        Entry(frame, justify=RIGHT, textvariable=self.WL).grid(row=9, column=3,
sticky=W)
        Entry(frame, justify=RIGHT, textvariable=self.H).grid(row=10, column=3,
sticky=W)

#Output Values
        Label(frame, text="Calculation Results:   The Factor of Safety is:
",bg='#FFB6C1').grid(row=15,column=1,sticky=E)
        Label(frame, textvariable=self.Fs,bg='#FFB6C1').grid(row=15, column=2,
sticky=W)
        Label(frame, textvariable=self.Result,bg='#FFB6C1').grid(row=15, column=3,
sticky=W)
        Label(frame, textvariable=self.Beta_notice,bg='#FFB6C1').grid(row=16, column=1,
sticky=W)
        Label(frame, textvariable=self.Beta_result,bg='#FFB6C1').grid(row=16, column=2,
sticky=W)
```

```
        Label(Lower_frame, textvariable=self.Notice,bg='#FFB6C1').grid(row=3,
column=2, sticky=W)


#Units
        Message(frame, text="m/s^2").grid(row=1, column=5)
        Message(frame, text="Unitless").grid(row=2, column=5)
        Message(frame, text="Unitless").grid(row=3, column=5)
        Message(frame, text="°").grid(row=4, column=5)
        Message(frame, text="Unitless").grid(row=5, column=5)
        Message(frame, text="Pa").grid(row=6, column=5)
        Message(frame, text="°").grid(row=7, column=5)
        Message(frame, text="°").grid(row=8, column=5)
        Message(frame, text="m").grid(row=9, column=5)
        Message(frame, text="m").grid(row=10, column=5)



        Frame(frame, height=10).grid(row=13, column=4, columnspan=7)


        # Button 1: Calculate
```

```
        Button(frame, width=19, text="Calculate",
command=self.calculate_1).grid(row=14, column=3)

        #Button 2: Select a File
        #Button(Lower_frame, width=19, text="Select A File",
command=self.read_variables).grid(row=2, column=2)

        # Button 3: Calculate whole file
        Button(Lower_frame, width=19, text="Calculate the whole file",
command=self.calculate_2).grid(row=6, column=2)

        window.mainloop()



# Main calculation of Button 1
    def calculate_1(self):
        #get values
        g = eval(self.g.get())
        e = eval(self.void_ratio.get())
        Gs= eval(self.specific_gravity.get())
```

```
Ybb  = eval(self.Yb.get()) #how to calculate

S = eval(self.Saturation.get())

c = eval(self.Effective_cohension.get())

YY = eval(self.Y.get())

T= eval(self.T.get())

WL  = eval(self.WL.get())

H  = eval(self.H.get())

Yb = Ybb/180*math.pi

Y = YY/180*math.pi

Theta = T/180*math.pi

if (Y+math.pi/2)/2 < Theta-0.17:

    Beta = [Y/2, (Y+math.pi/2)/2, Theta-0.17]

else:

    Beta = [Y/2, (Y/2+Theta-0.17)/2, Theta-0.17]

p=997

Yw=p

U =[0,0,0,0,0]

N=[]

I=[]

Fs=[1]
```

```
        Is=[]
        Fsf1 = [-1000000]
        Fsf=[]
        V=[]
        W=[]
        K=[]
        SS=[]
        P=[0,0,0,0,0]
        Sum_tol1 = 0
        Sum_tol2 = 0
        Sum_tol3 = 0

#first loop(different normal force)
        for l in range (3):
            LL =H/math.tan(Theta)
            h = LL* math.tan(Beta[l])
            h2 = H-h
            #kkk=0
            jj=0
            Level =H
```

```
            x = (h2/3)/math.tan(Beta[l])
            y = h2/3
            L1 = h2/math.sin(Beta[l])
            L2 = h/math.sin(Beta[l])
            L= [L1/3,L1/3,L1/3,L2/2,L2/2]
            L_tol = L[0]+L[1]+L[2]+L[3]+L[4]
#calculate the volume
            V.append(1/2*x*y)
            V.append(3/2*y*x)
            V.append(5/2*x*y)
            V.append(3/8*h2*LL)
            V.append(1/8*h2*LL)
            for i in range(5):
                if WL > Level:
                    self.Fs.set(format(0, '.3f'))
                    self.Result.set(format("Groundwater Level cant be higher than the
streambank"))
                else:
    # HYDROSTATIC FORCE
                    P_top=0
```

```
        P_Bot=(WL)*p*g

        Fw = (P_top+P_Bot)/2 * WL
# UPLIFTING FORCE

        U[0]=(WL-H+y/2)*Yw*L[0]*g

        U[1]=(WL-H+1.5*y)*Yw*L[1]*g

        U[2]=(WL-H+2.5*y)*Yw*L[2]*g

        U[3]=(WL-0.75*h)*Yw*L[3]*g

        U[4]=(WL-0.25*H)*Yw*L[4]*g


      Bulkdensity = Yw*(Gs+e*S)/(1+e)

      Weight = (V[i]* g * Bulkdensity)

      Normal_force= Weight/math.cos(Beta[l])

      Si=(1/Fs[0])*(L[i]*c+Normal_force*math.tan(Y)-U[i]*math.tan(Yb))

      Ks = (c*L[i]+Si*math.tan(Yb)-U[i]*math.tan(Y))/Fs[0]

      Kss = math.sin(Beta[l])-math.cos(Beta[l])*math.tan(Y)/Fs[0]

      if i==0:

        INJ = 0 - math.cos(Beta[l])*Ks + Normal_force * Kss

      else:

        INJ = I[i-1] - math.cos(Beta[l])*Ks+Normal_force * Kss

      ISJ = 0.4* INJ*math.sin((math.pi*(L[i]/L_tol))*math.pi/180)
```

```
            #print (Normal_force)
            #print (Ks)
            #print(Beta)
            if i==0:
                Normal_Force = (Weight-ISJ+0-
math.sin(Beta[l])*Ks)/(math.cos(Beta[l])+math.tan(Y)*math.sin(Beta[l])/Fs[0])
            else:
                Normal_Force = (Weight+Is[i-1]-ISJ-
math.sin(Beta[l])*Ks)/(math.cos(Beta[l])+math.tan(Y)*math.sin(Beta[l])/Fs[0])
            W.append(Weight)
            N.append(Normal_Force)
            K.append(Ks)
            Is.append(ISJ)
            I.append(INJ)
            SS.append(Si)
            #print(P)
            #print(U)
            #print(W)
            #print(Kss)
            #print(N)
```

```
            #print(Is)
            #print(I)
            #print(SS)
            Sum1 = c*L[i]+SS[i]*math.tan(Yb)+(Normal_force-U[i])*math.tan(Y)
            Sum2 = N[i]
            Sum_tol1+= Sum1
            Sum_tol2+= Sum2

        Fos = math.cos(Beta[l])*(Sum_tol1)/(math.sin(Beta[l])*Sum_tol2-Fw)
        Sum_tol2=0
        Sum_tol1=0
        #print(Fos)
        #print (Sum_tol1)
        #print(Sum_tol2)
        #print(Sum_tol3)
    #main loop, condition: error less than 0.1%, if the results cant meet the requiremnet, it
will continue running
        while abs((Fos-Fs[0])/Fs[0])>0.001:
            #print(Sum_tol1)
            Fs[0] = Fos
```

```
        for k in range (5):
            Si=(1/Fs[0])*(L[k]*c+N[k]*math.tan(Y)-U[k]*math.tan(Yb))
            Ks = (c*L[k]+Si*math.tan(Yb)-U[k]*math.tan(Y))/Fs[0]
            Kss = math.sin(Beta[l])-math.cos(Beta[l])*math.tan(Y)/Fs[0]
            if k==0:
                INJ = 0 - math.cos(Beta[l])*Ks + N[k] * Kss
            else:
                INJ = I[k-1] - math.cos(Beta[l])*Ks+N[k] * Kss
            ISJ = 0.4* INJ*math.sin((math.pi*(L[k]/L_tol))*math.pi/180)
            if k==0:
                Normal_Force = (W[k]-ISJ+0-
math.sin(Beta[l])*Ks)/(math.cos(Beta[l])+math.tan(Y)*math.sin(Beta[l])/Fs[0])
            else:
                Normal_Force = (W[k]+Is[k-1]-ISJ-
math.sin(Beta[l])*Ks)/(math.cos(Beta[l])+math.tan(Y)*math.sin(Beta[l])/Fs[0])
            Is[k]=ISJ
            I[k]=INJ
            SS[k] = Si
```

```
                Sum1 = c*L[k]+math.cos(Beta[l])+SS[k]*math.tan(Yb)+(N[k]-
U[k])*math.tan(Y)
                Sum2 = N[k]
                Sum_tol1+= Sum1
                Sum_tol2+= Sum2
                N[k]=Normal_Force
                #print (Sum_tol1)
            Fos = math.cos(Beta[l])*(Sum_tol1)/(math.sin(Beta[l])*Sum_tol2-Fw)
            Sum_tol2=0
            Sum_tol1=0
            jj+=1
            if jj >1000:
                break
            #print (jj)
            #print(Fs)
        Fsf.append(Fos)
        print (Fsf)
        print(Beta)
#Find the lowest Fs with Beta
    if Fsf[1]<Fsf[0] and Fsf[1]<Fsf[2]:
```

```
            a = ((Fsf[1]-Fsf[0])*(Beta[2]-Beta[1])-(Fsf[2]-Fsf[1])*(Beta[1]-
Beta[0]))/((Beta[1]*Beta[1]-Beta[0]*Beta[0])*(Beta[2]-Beta[1])-(Beta[2]*Beta[2]-
Beta[1]*Beta[1])*(Beta[1]-Beta[0]))
            b = (Fsf[1]-Fsf[0]-a*(Beta[1]*Beta[1]-Beta[0]*Beta[0]))/(Beta[1]-Beta[0])
            c = Fsf[0]-Beta[0]*Beta[0]*a-Beta[0]*b
            x_low = -b/(2*a)
            #print(a,b,c,x_low)
            y_low = (4*a*c-b*b)/(4*a)
            #print(y_low)
            Beta_results = x_low /math.pi*180
        elif Fsf[2]> Fsf[1] and Fsf[1]>Fsf[0]:
            y_low = Fsf[0]
            Beta_results = Beta[0]/math.pi*180
        elif Fsf[1]>Fsf[2] and Fsf[0]>Fsf[1]:
            y_low = Fsf[2]
            Beta_results = Beta[2]/math.pi*180
# OUTPUT
        if (y_low > 1):
            self.Fs.set(format(y_low, '.3f'))
            self.Result.set(format("The Streambank is Safe"))
```

```
            self.Beta_notice.set(format("The angle of the failure plane is"))
            self.Beta_result.set(format(Beta_results, '.3f'))
        elif (y_low< 1):
            self.Fs.set(format(y_low, '.3f'))
            self.Result.set(format("This Streambank is Unsafe"))
            self.Beta_result.set(format(Beta_results, '.3f'))
            self.Beta_notice.set(format("The angle of the failure plane is"))
        else:
            self.Fs.set(format(y_low, '.3f'))
            self.Result.set(format("This Streambank will Fail soon without any
intervention"))
            self.Beta_result.set(format(Beta_results, '.3f'))
            self.Beta_notice.set(format("The angle of the failure plane is"))
# select a file:
    #def browsefunc():
        #filename=askopenfile()
    #def open_file(self):
        #txt_file = askopenfile(title = "Select a file")
    def open_file(self):
```

```
        file = (filedialog.askopenfilename(title = 'Select a *.pm file',filetypes=[('text files',
'*.txt'),
        ('All files', '*.*')]))
        return file
    def open_file2(self):
        file = (filedialog.askopenfilename(title = 'Select a *.olf file',filetypes=[('text files',
'*.txt'),
        ('All files', '*.*')]))
        return file


# need a formatted input file
    def read_variables(self):
        """
        read data from txt
        :return:
        """
        txt_file = self.open_file()
        with open(txt_file, 'r', encoding='utf-8') as f:
            content = f.read()
```

```
        vars = re.findall('# [a-z A-Z\(\)\d]+', content)
        values = re.split('# [a-z A-Z\(\)\d]+', content)[1:]
        assert len(vars) == len(values)
        new_values = []
        for value in values:
            value = re.sub('[\n ]', ' ', value).strip().split()
            value = [float(v) for v in value]
            new_values.append(value.copy())

        return vars, new_values, value

# Calculate the whole file:
    def calculate_2(self):
        file = open ("C:/Program_Files/model_test.txt", 'a', encoding='utf-8')
        var_names, var_values, value = self.read_variables()
        X_cor = var_values[0]
        Y_cor = var_values[1]
        Z_cor = var_values[2]
        S =var_values[5]
        depth = var_values[6]
```

```
length = len(value)

g = eval(self.g.get())

e = eval(self.void_ratio.get())

Gs= eval(self.specific_gravity.get())

Ybb  = eval(self.Yb.get())

c = eval(self.Effective_cohension.get())

YY = eval(self.Y.get())

T= eval(self.T.get())

H  = eval(self.H.get())

Yb = Ybb/180*math.pi

Y = YY/180*math.pi

Theta = T/180*math.pi

if (Y+math.pi/2)/2 < Theta-0.17:

    Beta = [Y/2, (Y+math.pi/2)/2, Theta-0.17]

else:

    Beta = [Y/2, (Y/2+Theta-0.17)/2, Theta-0.17]

p=997

Yw=p

U =[0,0,0,0,0]
```

```
        N=[0,0,0,0,0]
        I=[0,0,0,0,0]
        Fs=[1]
        Is=[0,0,0,0,0]
        Fss = []
        Bett=[]
        Fsf1 = [-1000000]
        Fsf=[0,0,0]
        W=[0,0,0,0,0]
        K=[0,0,0,0,0]
        SS=[0,0,0,0,0]
        P=[0,0,0,0,0]
        Sum_tol1 = 0
        Sum_tol2 = 0
        Sum_tol3 = 0

#first loop(different normal force)
        for j in range (0, length):
            WL = depth[j]
            for l in range (0,3):
```

```
        LL =H/math.tan(Theta)
        h = LL* math.tan(Beta[l])
        h2 = H-h
        #kkk=0
        jj=0
        Level =H
        x = (h2/3)/math.tan(Beta[l])
        y = h2/3
        L1 = h2/math.sin(Beta[l])
        L2 = h/math.sin(Beta[l])
        L= [L1/3,L1/3,L1/3,L2/2,L2/2]
        L_tol = L[0]+L[1]+L[2]+L[3]+L[4]
        V =[1/2*x*y,3/2*y*x,5/2*x*y,3/8*h2*LL,1/8*h2*LL]
        for i in range(5):
# HYDROSTATIC FORCE
            P_top=0
            P_Bot=(WL)*p*g
            Fw = (P_top+P_Bot)/2 * WL
# UPLIFTING FORCE
            U[0]=(WL-H+y/2)*Yw*L[0]*g
```

```
U[1]=(WL-H+1.5*y)*Yw*L[1]*g

U[2]=(WL-H+2.5*y)*Yw*L[2]*g

U[3]=(WL-0.75*h)*Yw*L[3]*g

U[4]=(WL-0.25*H)*Yw*L[4]*g


Bulkdensity = Yw*(Gs+e*S[j])/(1+e)

Weight = (V[i]* g * Bulkdensity)

Normal_force= Weight/math.cos(Beta[l])

Si=(1/Fs[0])*(L[i]*c+Normal_force*math.tan(Y)-U[i]*math.tan(Yb))

Ks = (c*L[i]+Si*math.tan(Yb)-U[i]*math.tan(Y))/Fs[0]

Kss = math.sin(Beta[l])-math.cos(Beta[l])*math.tan(Y)/Fs[0]

if i==0:

   INJ = 0 - math.cos(Beta[l])*Ks + Normal_force * Kss

else:

   INJ = I[i-1] - math.cos(Beta[l])*Ks+Normal_force * Kss

ISJ = 0.4* INJ*math.sin((math.pi*(L[i]/L_tol))*math.pi/180)


if i==0:

   Normal_Force = (Weight-ISJ+0-

math.sin(Beta[l])*Ks)/(math.cos(Beta[l])+math.tan(Y)*math.sin(Beta[l])/Fs[0])
```

```
            else:
                Normal_Force = (Weight+Is[i-1]-ISJ-
math.sin(Beta[l])*Ks)/(math.cos(Beta[l])+math.tan(Y)*math.sin(Beta[l])/Fs[0])
            W[i] = Weight
            N[i] = Normal_Force
            K[i]=Ks
            Is[i] = ISJ
            I[i] = INJ
            SS[i] = Si
            Sum1 = c*L[i]+SS[i]*math.tan(Yb)+(Normal_force-U[i])*math.tan(Y)
            Sum2 = N[i]
            Sum_tol1+= Sum1
            Sum_tol2+= Sum2

        Fos = math.cos(Beta[l])*(Sum_tol1)/(math.sin(Beta[l])*Sum_tol2-Fw)
        Sum_tol2=0
        Sum_tol1=0
    #main loop, condition: error less than 0.1%, if the results cant meet the requiremnet, it
will continue running
        while abs((Fos-Fs[0])/Fs[0])>0.001:
```

```
            #print(Sum_tol1)
            Fs[0] = Fos
            for k in range (5):
                Si=(1/Fs[0])*(L[k]*c+N[k]*math.tan(Y)-U[k]*math.tan(Yb))
                Ks = (c*L[k]+Si*math.tan(Yb)-U[k]*math.tan(Y))/Fs[0]
                Kss = math.sin(Beta[l])-math.cos(Beta[l])*math.tan(Y)/Fs[0]
                if k==0:
                    INJ = 0 - math.cos(Beta[l])*Ks + N[k] * Kss
                else:
                    INJ = I[k-1] - math.cos(Beta[l])*Ks+N[k] * Kss
                ISJ = 0.4* INJ*math.sin((math.pi*(L[k]/L_tol))*math.pi/180)
                if k==0:
                    Normal_Force = (W[k]-ISJ+0-
math.sin(Beta[l])*Ks)/(math.cos(Beta[l])+math.tan(Y)*math.sin(Beta[l])/Fs[0])
                else:
                    Normal_Force = (W[k]+Is[k-1]-ISJ-
math.sin(Beta[l])*Ks)/(math.cos(Beta[l])+math.tan(Y)*math.sin(Beta[l])/Fs[0])
                Is[k]=ISJ
                I[k]=INJ
                SS[k] = Si
```

```
                Sum1 = c*L[k]+math.cos(Beta[l])+SS[k]*math.tan(Yb)+(N[k]-
U[k])*math.tan(Y)
                Sum2 = N[k]
                Sum_tol1+= Sum1
                Sum_tol2+= Sum2
                N[k]=Normal_Force
                #print (Sum_tol1)
            Fos = math.cos(Beta[l])*(Sum_tol1)/(math.sin(Beta[l])*Sum_tol2-Fw)
            Sum_tol2=0
            Sum_tol1=0
            jj+=1
            if jj >1000:
                break
        Fsf[l] = Fos
#Find the lowest Fs with Beta
    if Fsf[1]<Fsf[0] and Fsf[1]<Fsf[2] and Fsf[1] >0:
        a = ((Fsf[1]-Fsf[0])*(Beta[2]-Beta[1])-(Fsf[2]-Fsf[1])*(Beta[1]-
Beta[0]))/((Beta[1]*Beta[1]-Beta[0]*Beta[0])*(Beta[2]-Beta[1])-(Beta[2]*Beta[2]-
Beta[1]*Beta[1])*(Beta[1]-Beta[0]))
        b = (Fsf[1]-Fsf[0]-a*(Beta[1]*Beta[1]-Beta[0]*Beta[0]))/(Beta[1]-Beta[0])
```

```
            c = Fsf[0]-Beta[0]*Beta[0]*a-Beta[0]*b
            x_low = -b/(2*a)
            #print(a,b,c,x_low)
            y_low = (4*a*c-b*b)/(4*a)
            #print(y_low)
            Beta_results = x_low /math.pi*180
        elif Fsf[2]> Fsf[1] and Fsf[1]>Fsf[0] and Fsf[0] >0:
            y_low = Fsf[0]
            Beta_results = Beta[0]/math.pi*180
        elif Fsf[1]>Fsf[2] and Fsf[0]>Fsf[1] and Fsf[2] >0:
            y_low = Fsf[2]
            Beta_results = Beta[2]/math.pi*180
        else:
            y_low = 0
            Beta_results = 0
        Fss.append(y_low)
        Bett.append(Beta_results)
    file.write('\n'+"# Fs"+'\n')
    le = len(Fss)
    for m in range (le):
```

```
    if (m+1)%5 !=0:
        file.write(str(Fss[m])+'       ')
    else:
        file.write(str(Fss[m])+'\n')
    j+=1
    print (j)
wk=xlwt.Workbook(encoding='utf-8',style_compression=0)
sht = wk.add_sheet("sheet1",cell_overwrite_ok=True)
sht.write(0,0,'X')
sht.write(0,1,'Y')
sht.write(0,2,'Z')
sht.write(0,3,'Saturation')
sht.write(0,4,'Fs')
sht.write(0,5,'Beta')
for m in range (le):
    sht.write (m+1,0,X_cor[m])
    sht.write (m+1,1,Y_cor[m])
    sht.write (m+1,2,Z_cor[m])
    sht.write (m+1,3,S[m])
    sht.write (m+1,4,Fss[m])
```

```
            sht.write (m+1,5,Bett[m])
        wk.save('C:/Program_Files/output_file.csv')
        self.Notice.set(format("Finshed, file location:C:/Program_Files/output_file"))



#Menu
def about():
    dialog.showinfo(title='About', message = "This is a software for calculting the factor of
safety, Author: Quan Wei, Version 4.0" )
def help():
    dialog.showinfo(title='Help', message = "Please read carefully: if you want to use it as
an individual calculation, please use the top frame, and if you want to calculate the whole
file, please use the excel format provided and use the lower frame" )
menubar = Menu(window)


menubar.add_command(label="About",command=about)
menubar.add_command(label="Help",command=help)
menubar.add_command(label="Quit",command=window.quit)
window.config(menu=menubar)
```

```
if __name__ == '__main__':
    Calculator()
    pass
```